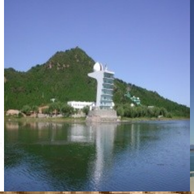

Observation on Current Helicity and Proxies of Subsurface Kinetic Helicity in Solar Active Regions

Gao Yu

Under instruction or Collaborated with:

Zhang, H. Q., Xu, H. Q., …

Sokoloff, D., Kuzanyan, K., …

Sakurai, T., …

Zhao, J.

α-Ω Dynamo Model

$$\frac{\partial A}{\partial t} = \alpha B + \frac{1}{\mu\sigma}\nabla^2 A$$

$$\frac{\partial B}{\partial t} = \nabla\times\left[v\times\left(\nabla\times A\right)\right] + \frac{1}{\mu\sigma}\nabla^2 B$$

$$\alpha = \alpha^k + \alpha^M \sim -\frac{\tau}{3}\vec{v}\times(\nabla\times\vec{v}) + \frac{\tau}{12\pi\rho}\vec{B}\times(\nabla\times\vec{B})$$

Refer to Parker, E. N. 1955; Frisch et al., 1975, Pouquet, 1976; Kleeorin, et al. 2003 … .

Vector field, both magnetic and velocity field, are new type measurements in the studies of solar observation, but convenient tools for computing helicity.

Systematic Observational Characteristic of Heli city in Active Regions

Hemispheric Helicity Sign Rule (HSR): In the northern (southern) solar hemisphere, the helicity mainly possesses left (right) handedness (Seehafer 1990; Pevtsov et al. 1995; Abramenko, et al., 1996; Wang et al. 1996; Bao and Zhang 1998; Hagino and Sakurai 2004, 2005; Zhang et al. 2010; Hao and Zhang 2012, Liu, Hoeksema, Sun 2014);

Observed helicity may indicate different sources of generation because the HSR shows a big scatter.(Bao and Zhang 2000; Kuzanyan et al. 2003);

HSR may change during some phase of solar cycle (e.g.,Bao and Zhang, 2000; Hagino and Sakurai 2005; Zhang et al. 2010);

HSR in different region of field strength exhibits opposite sign-preference (Zhang 2006; Hao and Zhang 2012; Otsuji, Sakurai, and Kuzanyan, 2015; Seligman, Petrie, and Komm 2014).

…

Turbulence of the flow in the solar convection zone may play important role for such diversely observational property.

Theoretical Analyses Combined with Systematic Observation Over Solar Cycles

Current helicity and magnetic field anisotropy in solar active regions (Xu, H. et al. 2015);

The origin of the helicity hemispheric sign rule reversals in the mean-field solar-type dynamo (Pipin, V. V. et al. 2013);

Current Helicity of Active Regions as a Tracer of Large-scale Solar Magnetic Helicity (Zhang, H. et al. 2012);

Current Helicity and Twist as Two Indicators of the Mirror Asymmetry of Solar Magnetic Fields (Sokoloff, D. et al. 2008);

Magnetic helicity evolution during the solar activity cycle: Observations and dynamo theory (Kleeorin, N. et al., 2003).

Aims of my following parts are:

1) Exhibit some properties of current helicity obtained with vector magnetic field;
2) Check the connection between current and subsurface kinetic helicity;
3) Exhibit some properties of subsurface vorticity and divergence obtained with vector velocity Field.

Definition of Main Parameters

Vertical electric current, current helicity and average force free field factor (Seehafer 1990; Pevtsov et al. 1995; Abramenko, et al., 1996; Wang et al. 1996; Bao and Zhang 1998; Hagino and Sakurai 2004, 2005):

$$J_z = \frac{1}{\mu_0}(\nabla \times B)_z,$$

$$H_c = B_z \times (\nabla \times B)_z,$$

$$\alpha_{av} = \frac{\sum (\nabla \times B)_z \times sign[B_z]}{\sum |B_z|}$$

The other processing was kept consistent with Bao and Zhang (1998).

Evolution of Spatial Distribution of Current Helicity over Two Cycles

Q: How about helicity distribution over two adjacent solar cycles?

Average helicity values over 7 degree and overlapping two year period;

95% confidence interval is given by taking each measured point as a freedom degree;

The HSR percentage is about 66% (63%) in the 22nd cycle and 58% (57%) in the 23rd cycle.

Zhang, Sakurai, Pevtsov, Gao, Xu, Sokoloff & Kuzanyan 2010, MNRAS

Calibration of field is dependent with wavelength, but for application to helicity one is often interested in spatial variation.

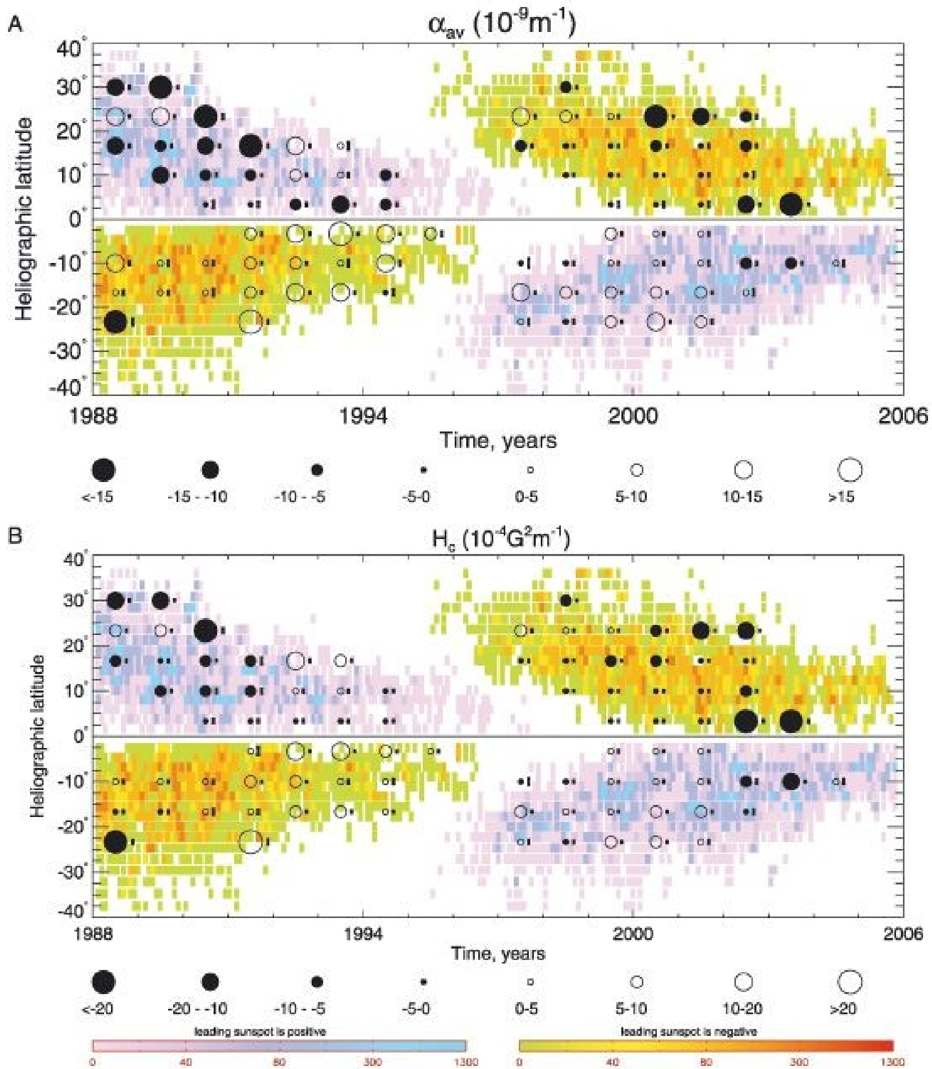

Analysis of Faraday Rotation

Scanning range □
-150 mÅ – 150 mÅ
 Step □ 10 mÅ
2003-04-04 □ NOAA AR 10325
Location: (11.7°, 17.6°);
2003-06-09 □ NOAA AR 10377
Location : (5.4°, -9.9°);
2003-10-23 □ NOAA AR 10484
Location : (4.0°, -12.5°) □

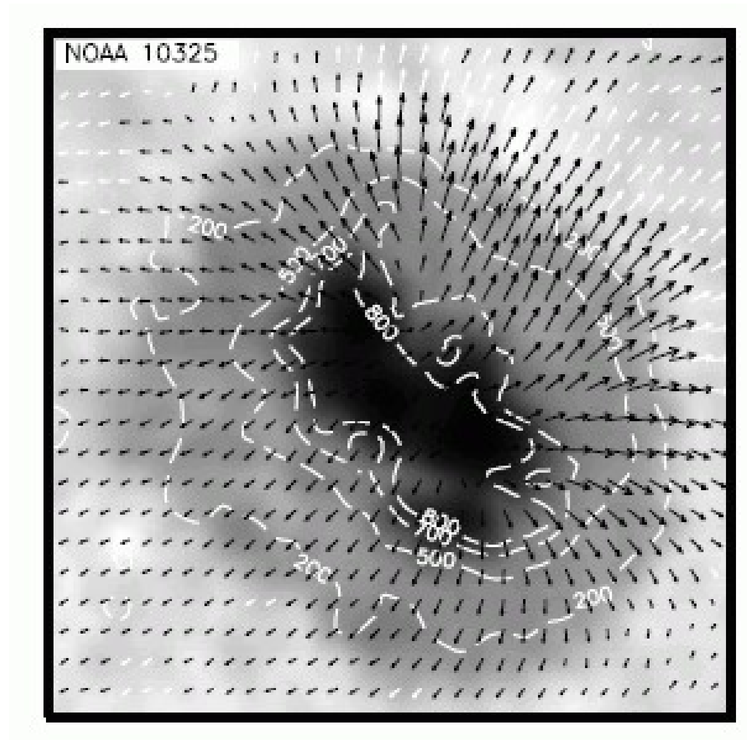

Su and Zhang (2004a, b)

A key assumption
:

take into account t
hose correlated az
imuths between m
easurements at ce
nter and wing of s
pectral line.

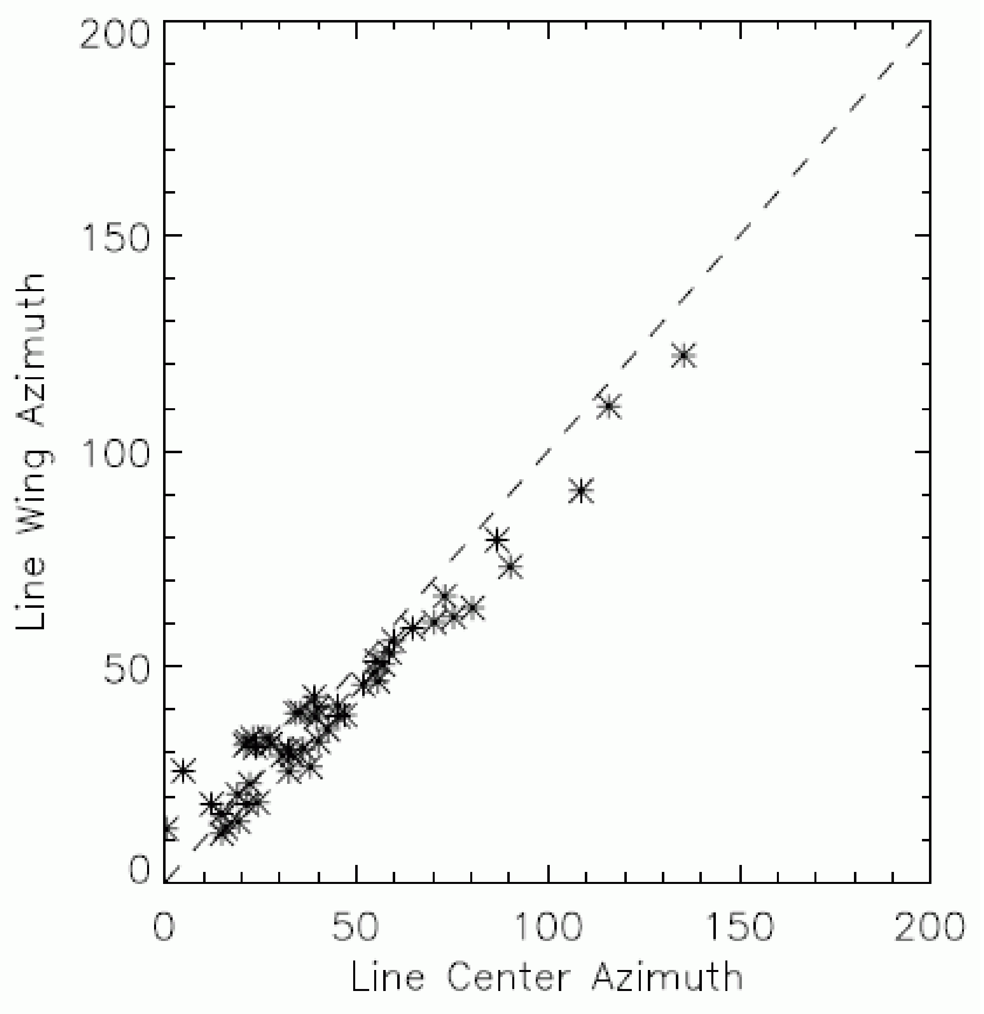

Azimuth Rotation in three Data Samples

B_z (G)	$\overline{\delta\phi} \pm \sigma$		
	10,325	10,484	10,377
200–300	$-2.7° \pm 8.5°$	$3.4° \pm 8.8°$	$4° \pm 19°$
300-400	$0.9° \pm 7.4°$	$3.4° \pm 7.8°$	$3° \pm 14°$
400–500	$3.9° \pm 5.4°$	$4.0° \pm 6.8°$	$4° \pm 10°$
500–600	$5.0° \pm 5.4°$	$5.7° \pm 6.5°$	$6° \pm 12°$
600–700	$6.2° \pm 6.1°$	$7.1° \pm 7.4°$	$7° \pm 13°$
700–800	$5.9° \pm 9.3°$	$8.6° \pm 8.3°$	$13° \pm 13°$

Azimuthal Rotations Caused by Faraday Effects with Field Strength and Inclination

	$\overline{\Delta\delta\phi} \pm \sigma$ (°)						
				B_z(G)			
ψ (°)	200–300 (per cent)	300–400 (per cent)	400–500 (per cent)	500–600 (per cent)	600–700 (per cent)	700–800 (per cent)	800–900 (per cent)
72–75	2.4 ± 4.1(2.7)						
69–72	3.3 ± 4.2(1.7)	4.1 ± 3.7(3.4)					
66–69	3.4 ± 5.9(1.4)	4.0 ± 3.7(3.2)	5.7 ± 3.0(4.9)				
63–66		4.1 ± 5.0(2.4)	5.2 ± 3.6(3.7)	6.0 ± 3.3(3.7)			
60–63		5.5 ± 4.7(1.7)	4.8 ± 3.8(3.5)	6.4 ± 3.7(6.1)	6.9 ± 3.9(1.6)		
57–60			5.0 ± 4.2(2.4)	5.3 ± 4.9(4.7)	7.5 ± 5.5(5.3)		
54–57			6.0 ± 5.0(1.2)	4.3 ± 6.5(3.9)	7.8 ± 7.0(4.9)		
51–54				7.5 ± 8.4(2.2)	8.6 ± 6.9(4.5)	8.5 ± 6.6(3.4)	
48–51					7.3 ± 6.7(2.8)	9.9 ± 6.3(5.6)	10.8 ± 4.5(1.3)
45–48						9.3 ± 6.5(3.3)	10.3 ± 5.7(3.0)
42–45						7.9 ± 10.5(1.8)	9.5 ± 7.3(2.1)

Gao, Y., Su, J. T., Xu, H. Q., and Zhang, H. Q., 2008

Electric Current in Strong Field Region

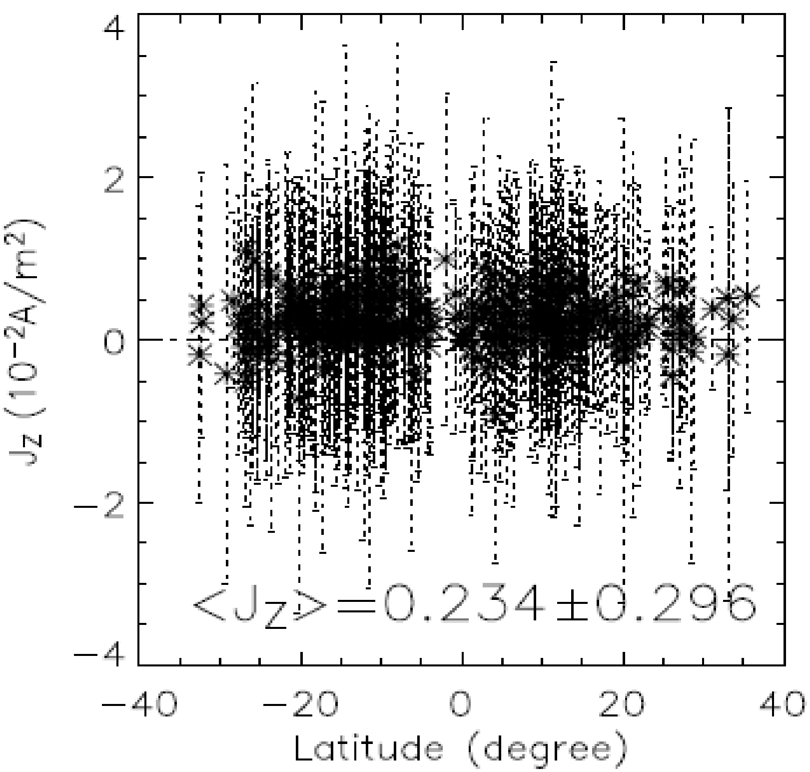

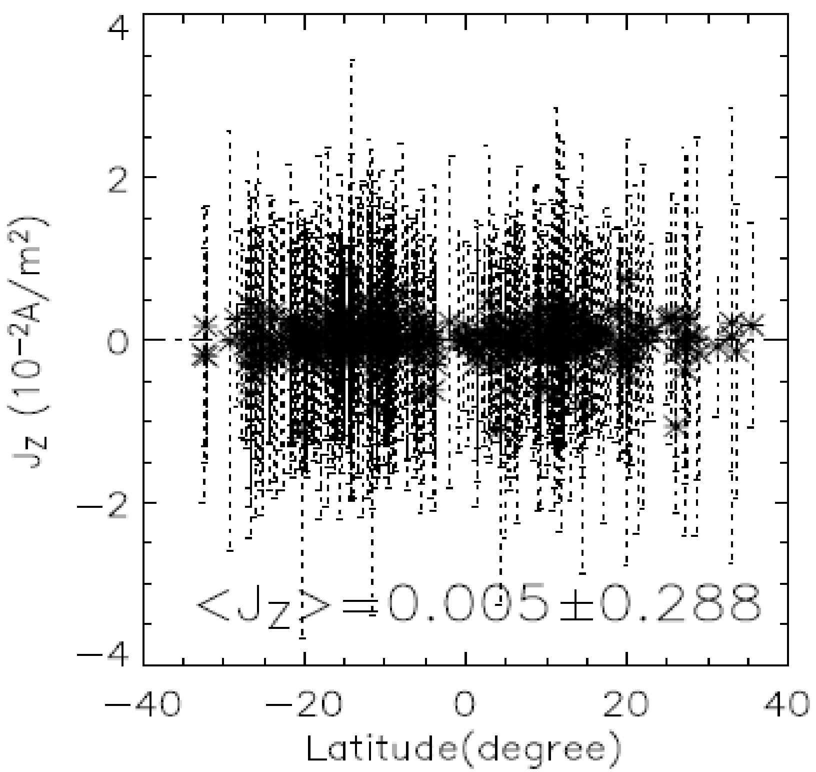

Latitudinal Distribution of Mean Current Helicity of ARs in 22nd and 23rd Solar Cycles

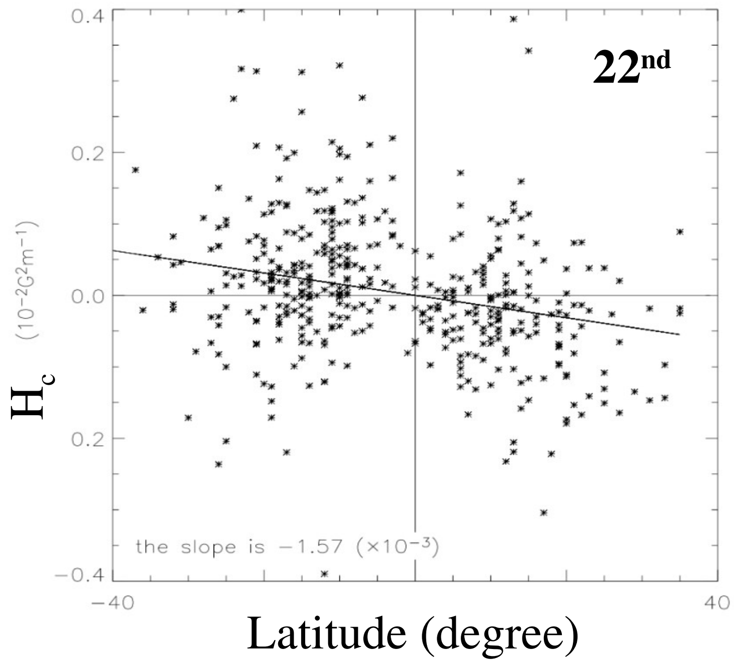

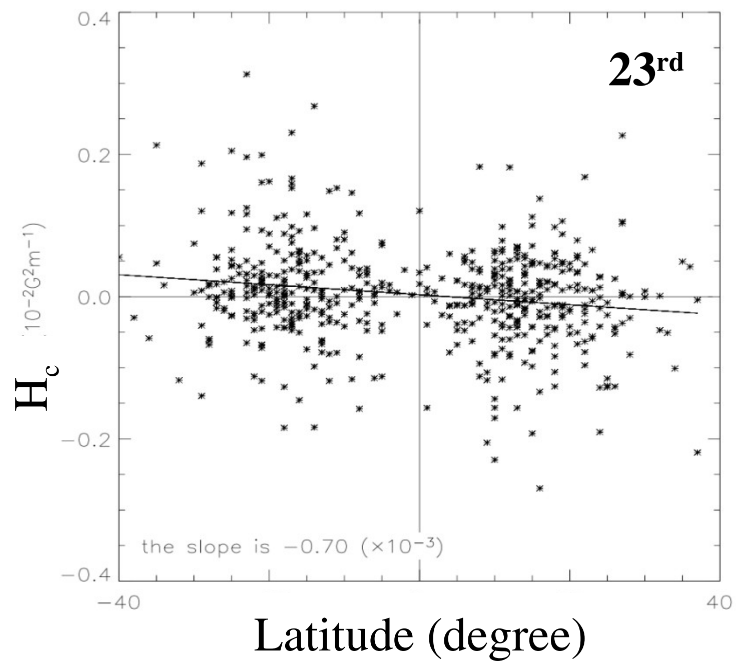

In this study (Gao et al. 2008), 984 active regions (6205 magnetograms in all) have been selected from 1988 to 2005, in which 431 active regions are in the 22nd solar cycle and 553 active regions are in the 23rd solar cycle.

Normal Probability Paper Applied for Distribution of Current Helicity

Q: Is there different ingredients since we have seen big scatter of the HSR?

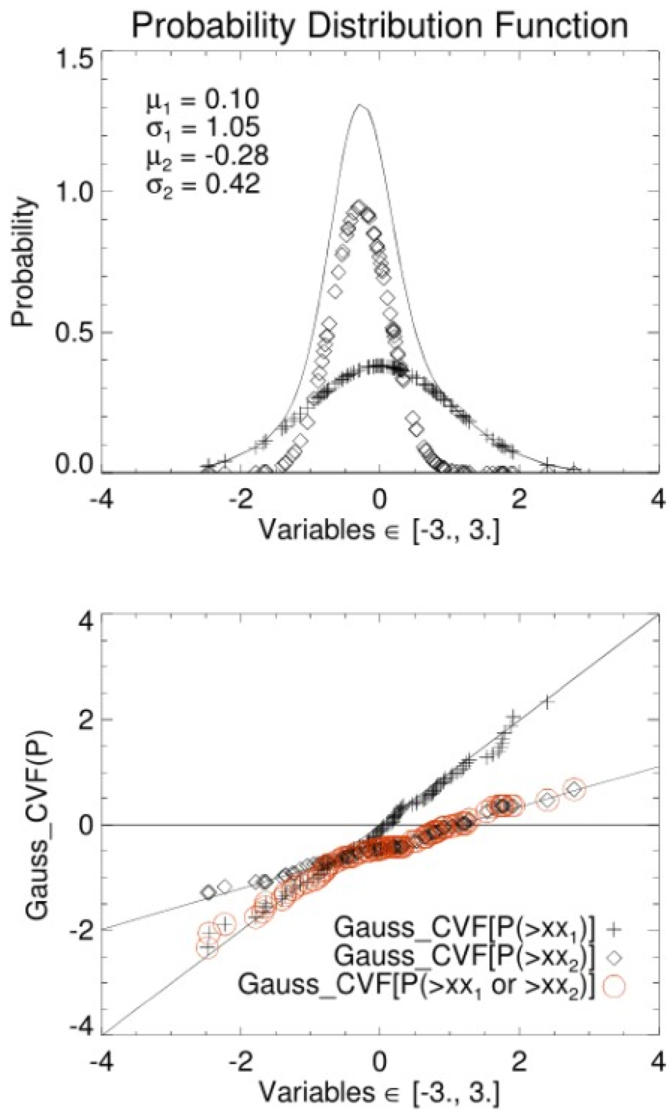

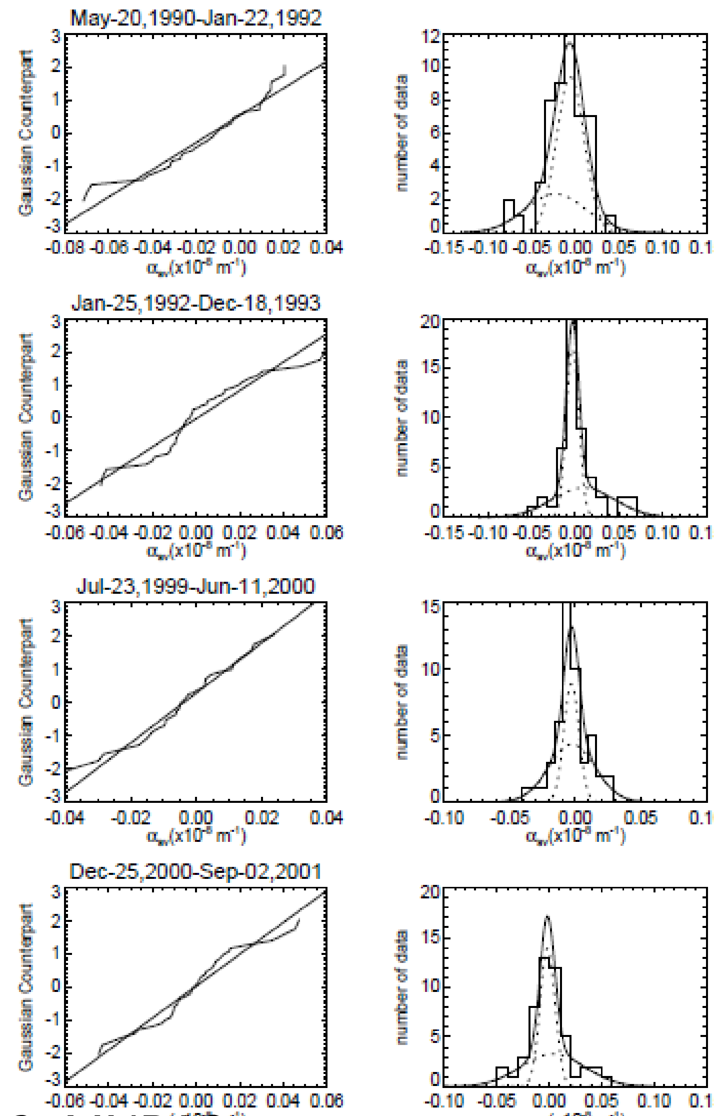

Gao, Sakurai, Zhang, Kuzanyan & Sokoloff 2012, MNRAS

Bins of Statistically Significant in Butterfly Diagram

♯	Start	End	μ_1	$\frac{\sigma_1 t_{n-5}}{\sqrt{n-5}}$	μ_2	$\frac{\sigma_2 t_{n-5}}{\sqrt{n-5}}$
3	Jan-25,1992	Dec-18,1993	-0.0031	0.0018	**0.0094**	0.0088
8	Dec-25,2000	Sep-02,2001	**0.0035**	0.0077	-0.0015	0.0018
9	Sep-22,2001	Jun-28,2003	-0.0045	0.0042	**0.2665**	0.0769
10	Jul-5,2003	Dec-23,2005	-0.0057	0.0129	**0.0008**	0.0021

♯	Start	End	μ_1	$\frac{\sigma_1 t_{n-5}}{\sqrt{n-5}}$	μ_2	$\frac{\sigma_2 t_{n-5}}{\sqrt{n-5}}$
1	Apr-26,1988	Feb-25,1990	**-0.0003**	0.0045	**-0.0227**	0.0122
5	Jul-29,1993	Aug-27,1996	**-0.0019**	0.0026	0.0147	0.0070
7	May-19,1999	Apr-12,2000	**-0.0001**	0.0023	**-0.0587**	0.0014
10	Oct-22,2001	Oct-27,2003	0.0017	0.0041	**-0.0694**	0.0010
11	Oct-28,2003	Dec-16,2005	**-0.0070**	0.0136	0.0010	0.0042

♯	Start	End	μ_1	$\frac{\sigma_1 t_{n-5}}{\sqrt{n-5}}$	μ_2	$\frac{\sigma_2 t_{n-5}}{\sqrt{n-5}}$
3	Jan-25,1992	Dec-18,1993	**0.0157**	0.0288	**0.5670**	0.2500

♯	Start	End	μ_1	$\frac{\sigma_1 t_{n-5}}{\sqrt{n-5}}$	μ_2	$\frac{\sigma_2 t_{n-5}}{\sqrt{n-5}}$
1	Apr-26,1988	Feb-25,1990	**-0.0004**	0.0252	**-0.8515**	0.0259
7	May-19,1999	Apr-12,2000	**-0.0045**	0.0097	0.0317	0.0322
11	Oct-28,2003	Dec-16,2005	**-0.0173**	0.0544	**-0.4921**	0.2334

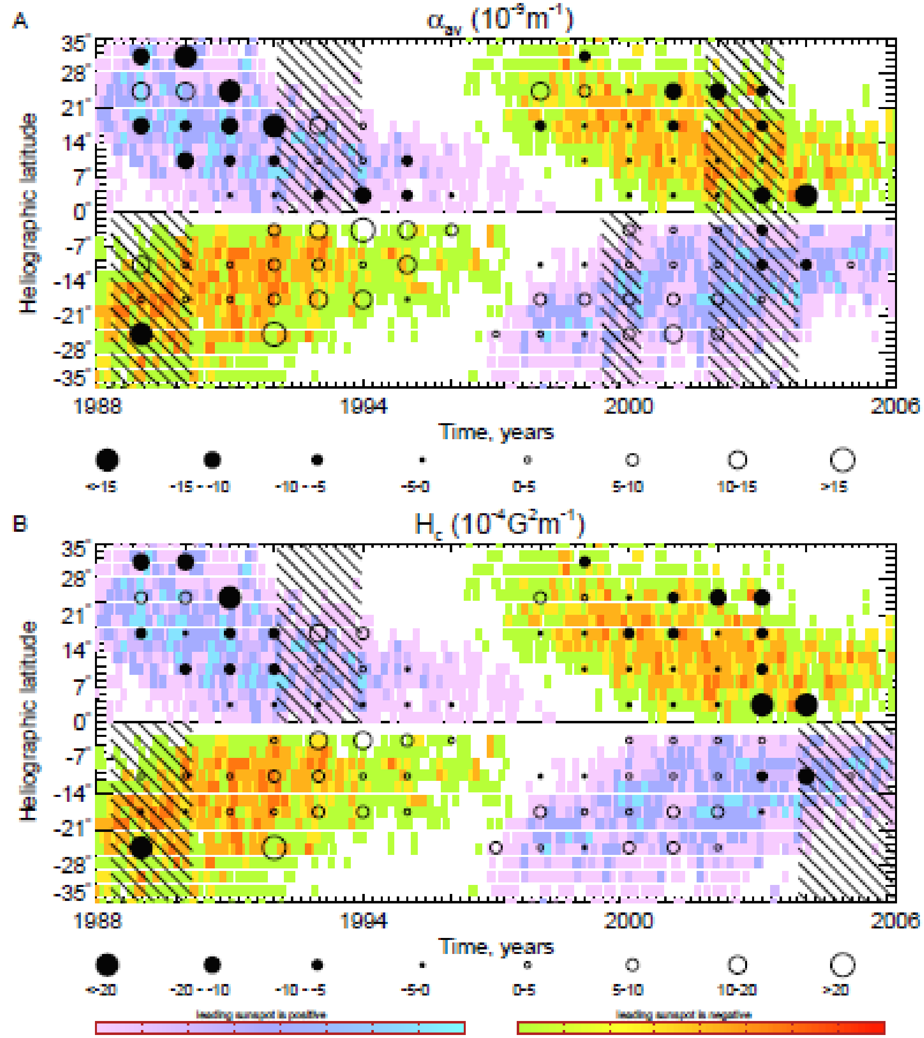

Butterfly Diagram of Net Current

Net current in opposite po larities conforms with the Hemispheric Sign Rule o btained with other helicity proxies.

Gao, Y. 2013, RAA.

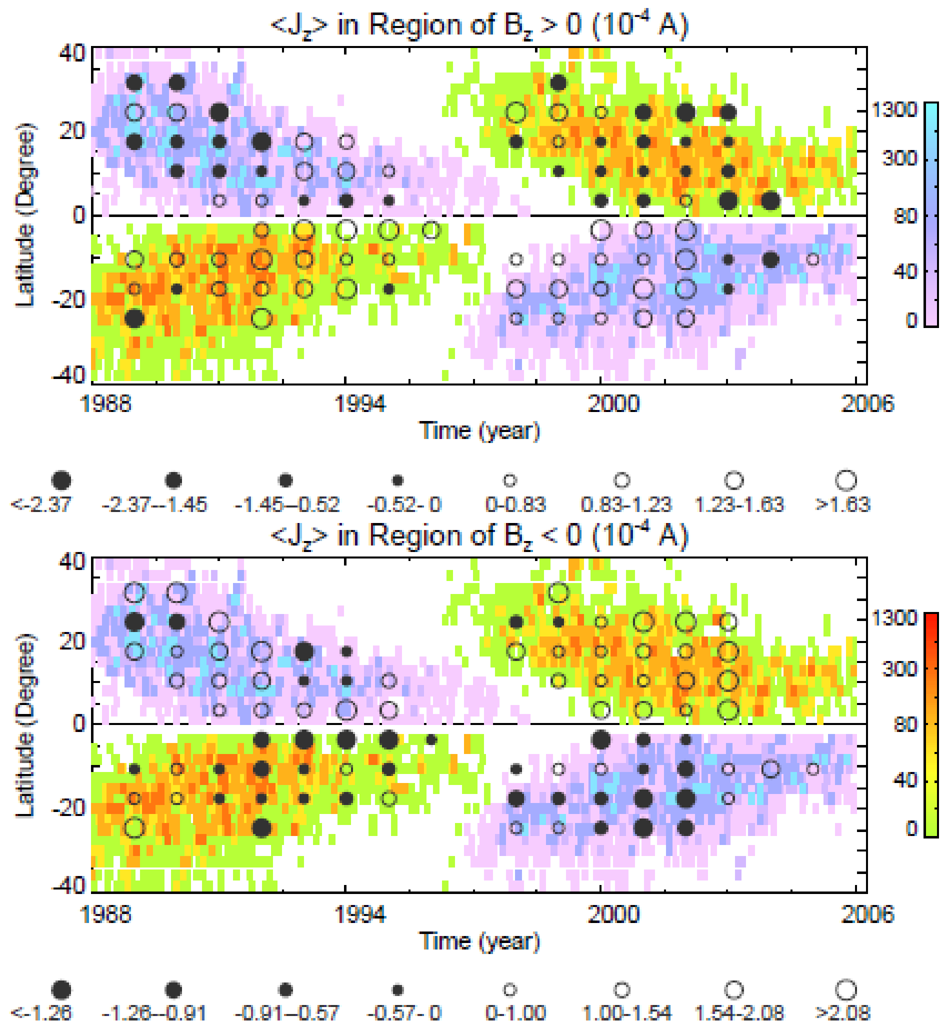

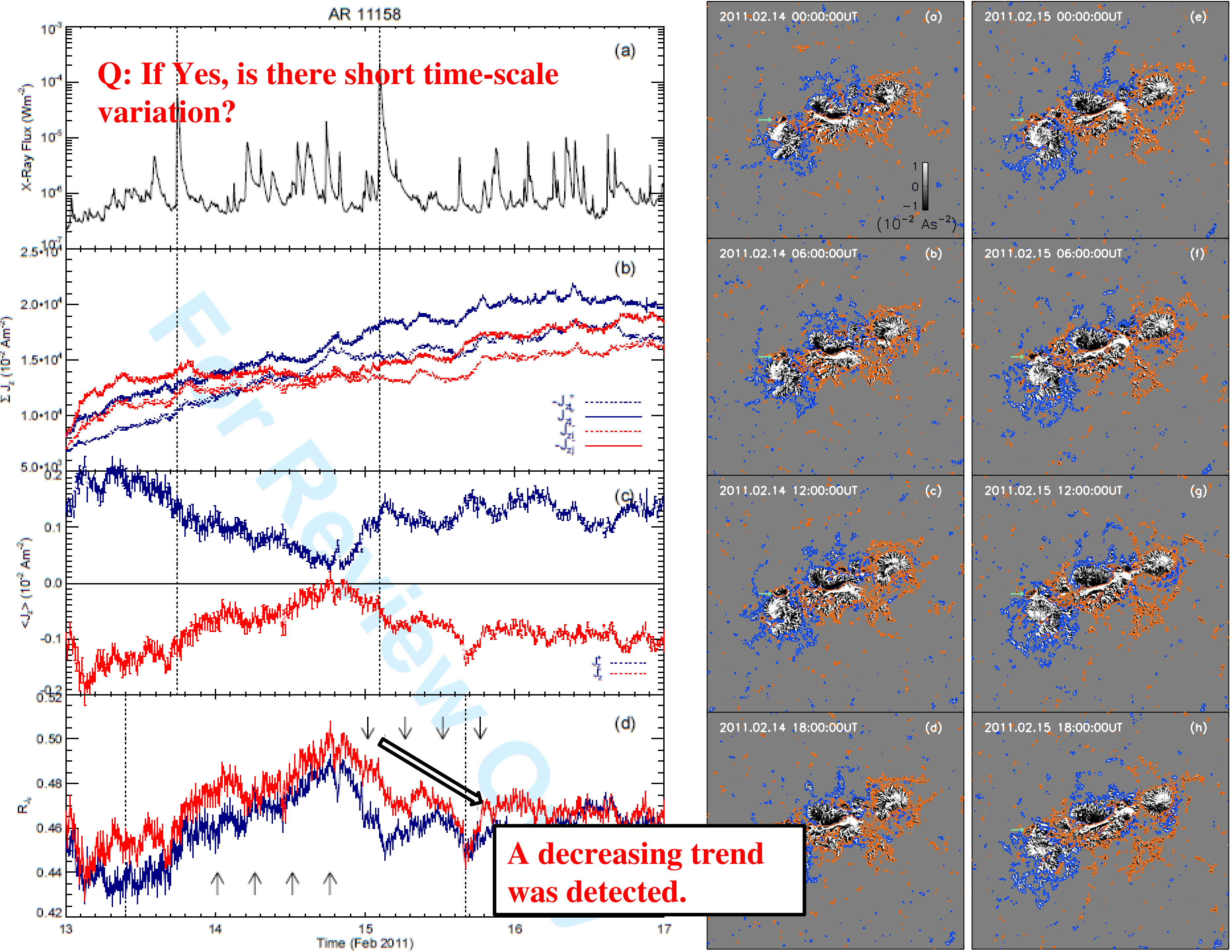
AR 11158
Q: If Yes, is there short time-scale variation?
A decreasing trend was detected.
(a)
(b)
(c)
(d)
X-Ray Flux (Wm^{-2})
ΣJ_z (10^{-2} Am^{-2})
$<J_z>$ (10^{-2} Am^{-2})
R_{J_z}
Time (Feb 2011)
2011.02.14 00:00:00UT (a)
2011.02.14 06:00:00UT (b)
2011.02.14 12:00:00UT (c)
2011.02.14 18:00:00UT (d)
2011.02.15 00:00:00UT (e)
2011.02.15 06:00:00UT (f)
2011.02.15 12:00:00UT (g)
2011.02.15 18:00:00UT (h)
(10^{-2} As^{-2})

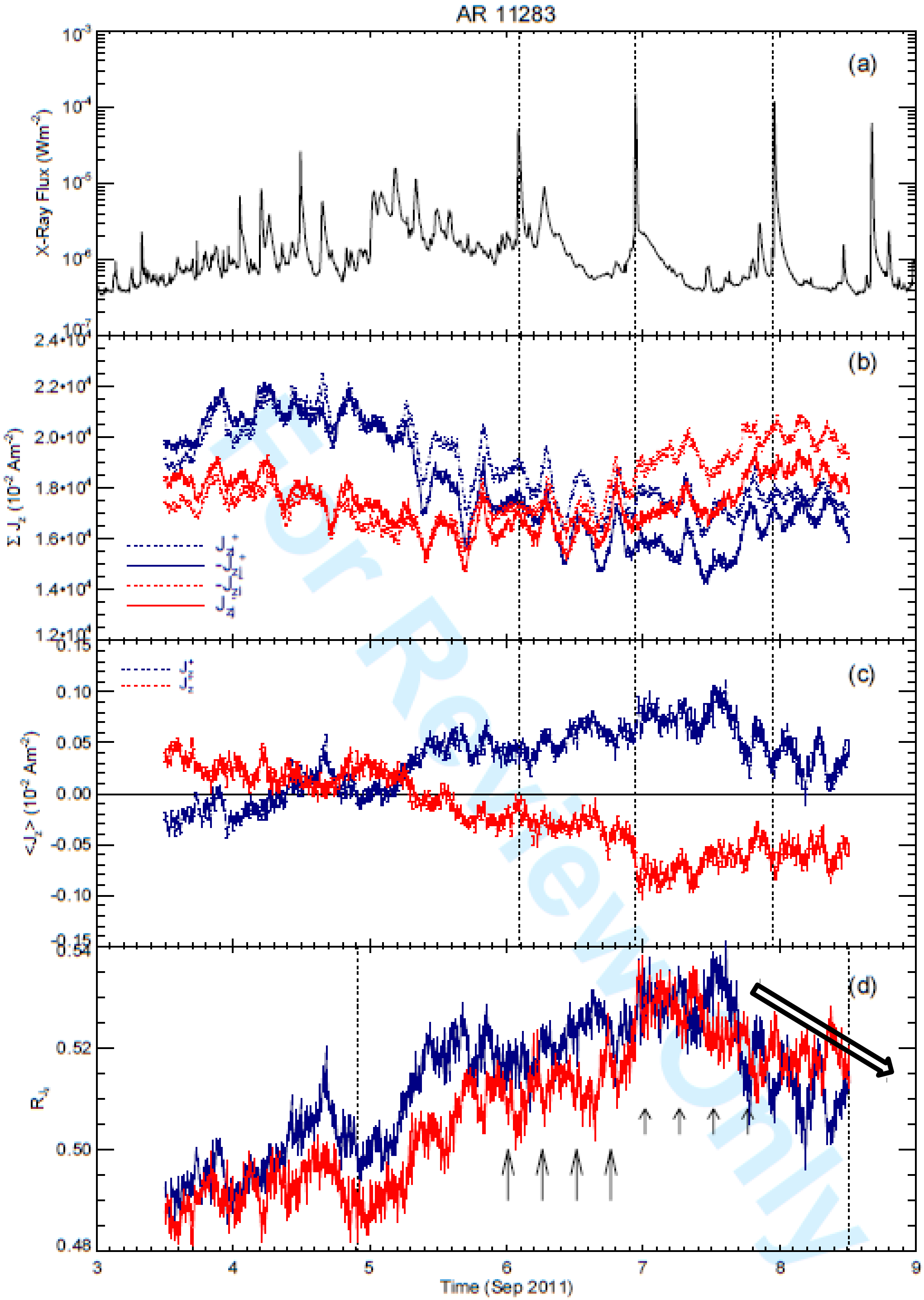
AR 11283
(a)
X-Ray Flux (Wm^{-2})
(b)
Σ J_z (10^{-2} Am^{-2})
(c)
<J_z> (10^{-2} Am^{-2})
(d)
R_{J_z}
Time (Sep 2011)

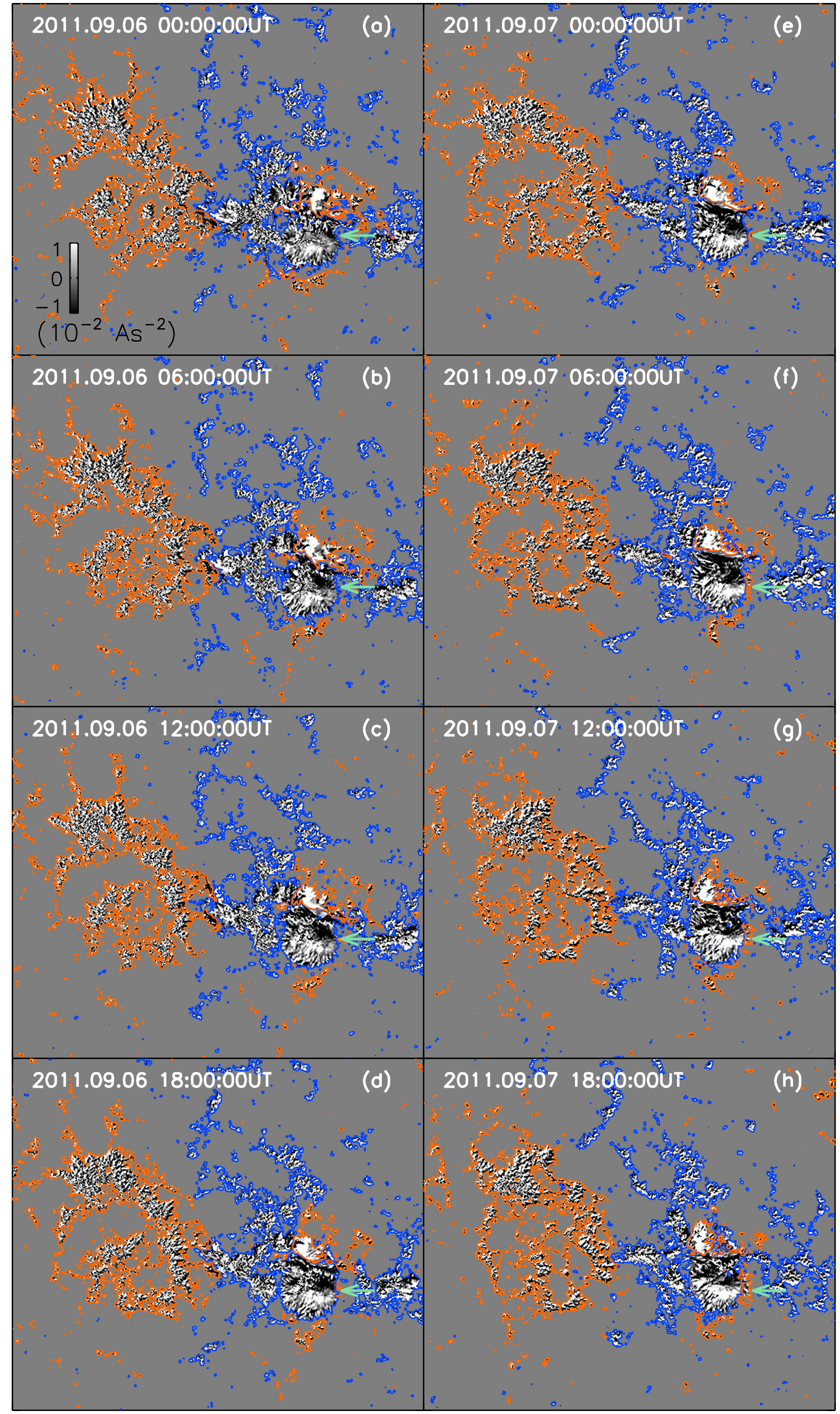
2011.09.06 00:00:00UT (a)
2011.09.07 00:00:00UT (e)
2011.09.06 06:00:00UT (b)
2011.09.07 06:00:00UT (f)
2011.09.06 12:00:00UT (c)
2011.09.07 12:00:00UT (g)
2011.09.06 18:00:00UT (d)
2011.09.07 18:00:00UT (h)
(10^{-2} As^{-2})

Mean Magnetic Field Quantities

Q: What else can we see from vector magnetic field if they are related with dynamo?

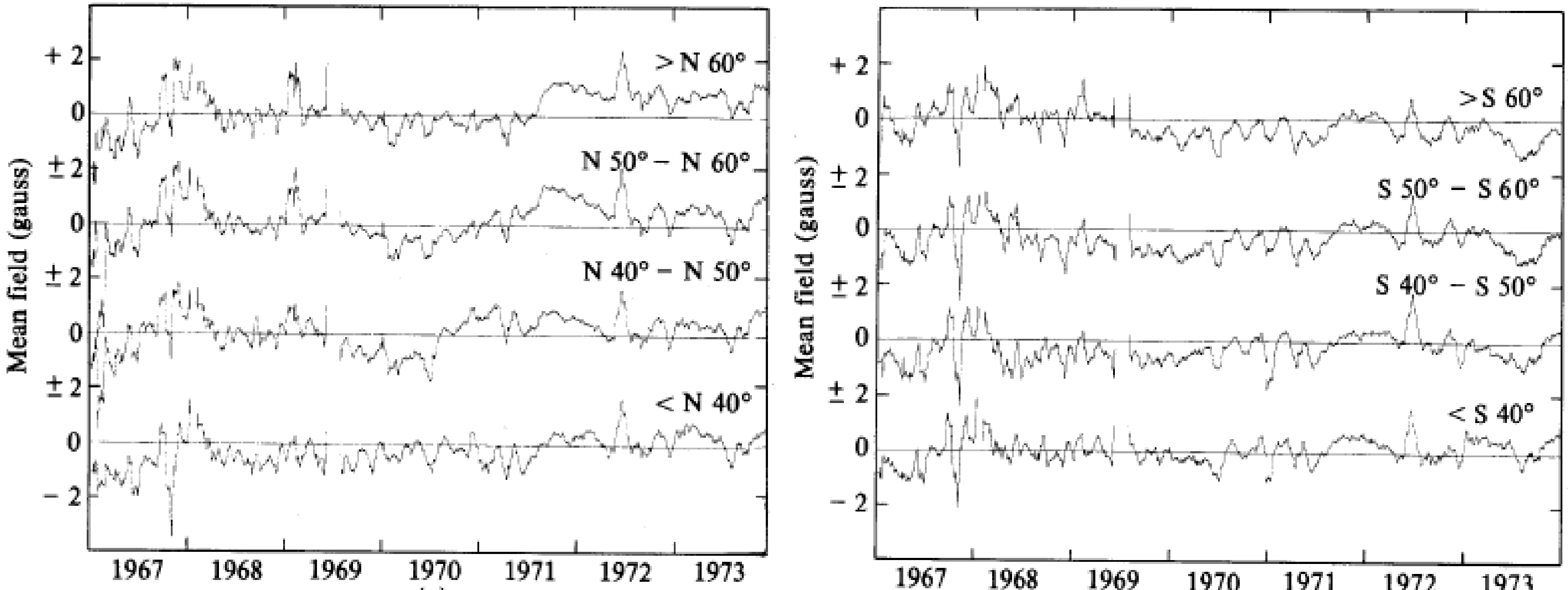

nent of the Sun's surface magnetic field, averaged over bands of latitude, and smoothed over the 27-day rotation period. (*a*) Northern hemisphere. (*b*) Southern hemisphere. (From Howard, 1974.)

H. K. Moffatt, 1978, Magnetic Field Generation In Electrically Conducting Fluids, Cambridge University Press.

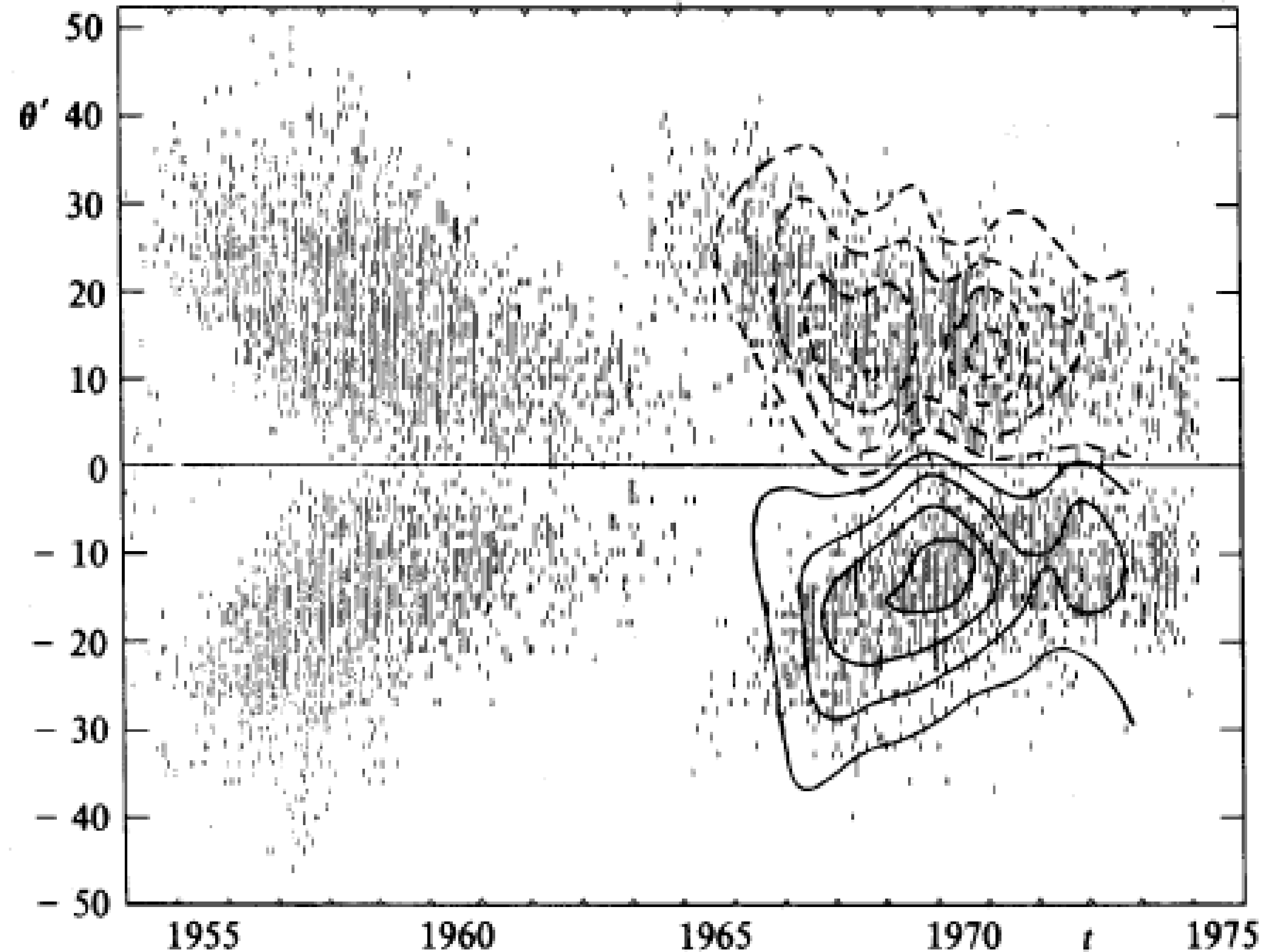

Fig. 5.5 Butterfly diagram for 1954 to 1975 (Mt. Wilson Observatory) and contours of constant radial field component. The levels of the curves are approximately ±0·17, ±0·50, ±0·83 and ±1·16 gauss, positive for the solid and negative for the dashed curves. (From Stix, 1976.)

Sign Preference of Three Components of Vector Magnetic Field with Solar Cycle

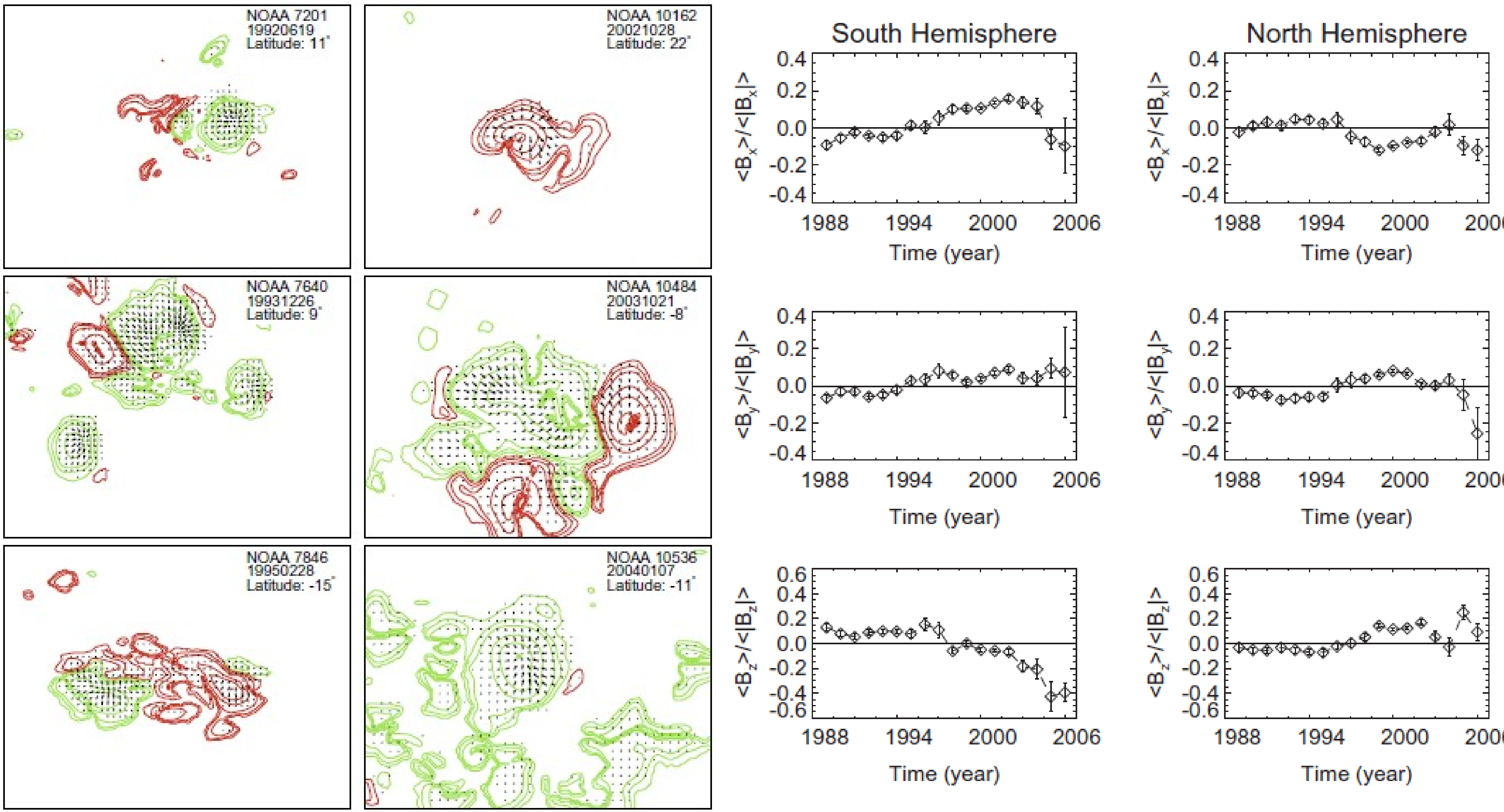

Sign preferences of vector magnetic field with time and hemisphere are found. ***Gao, Y., 2011***

In form of Butterfly Diagrams

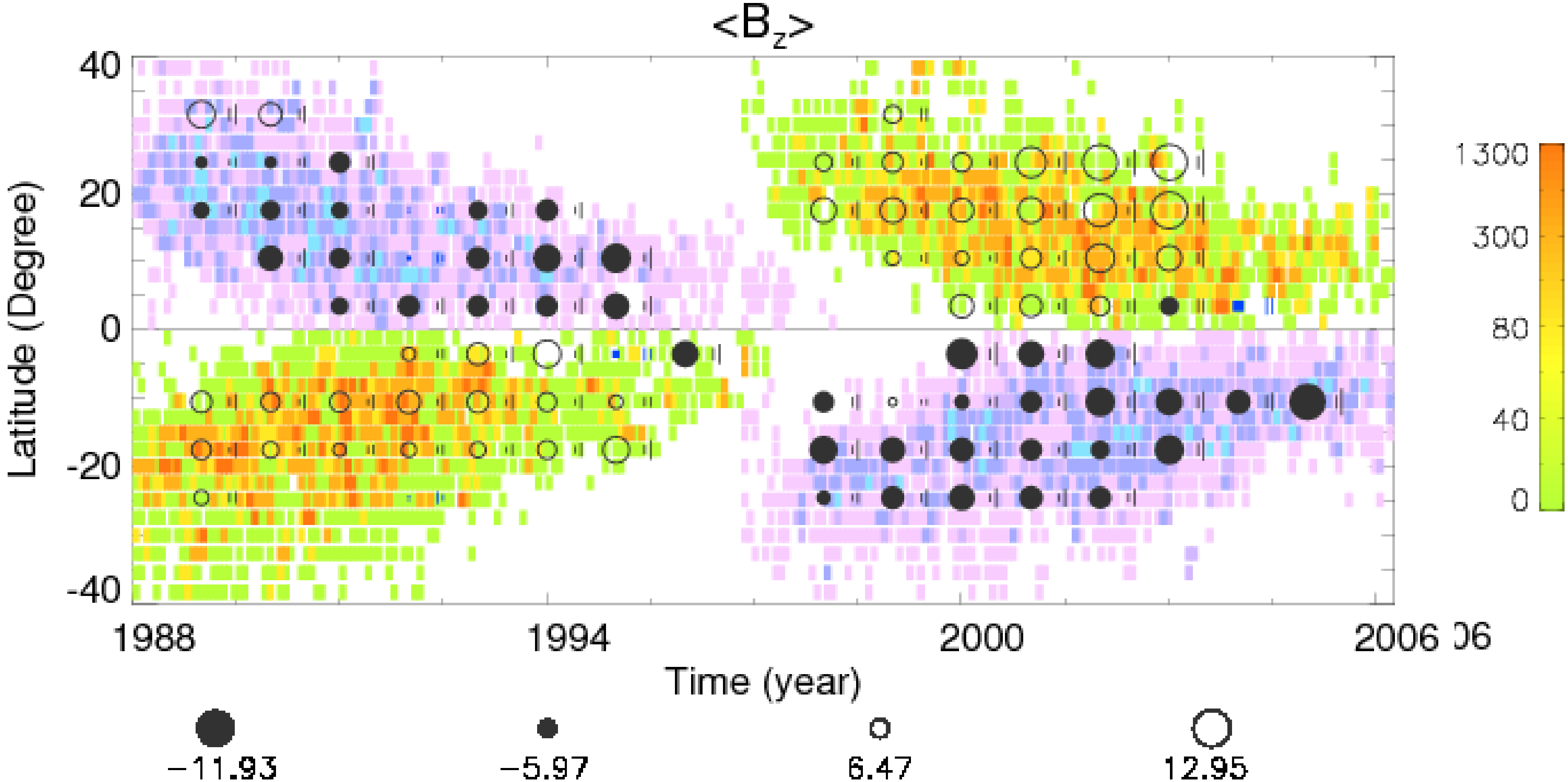

Distribution of residuals of vector magnetic field over active region.

Pre-SDO/HMI Comparison between Two Kinds of Heli city

The one-to-one statistical comparison between the current and subsurface kinetic helicity of sampling active regions has been performed (Zhao and Kosovichev 2003; Zhao 2004.; Gao, Zhang and Zhao, 2008; Maurya, Ambastha and Reddy 2011).

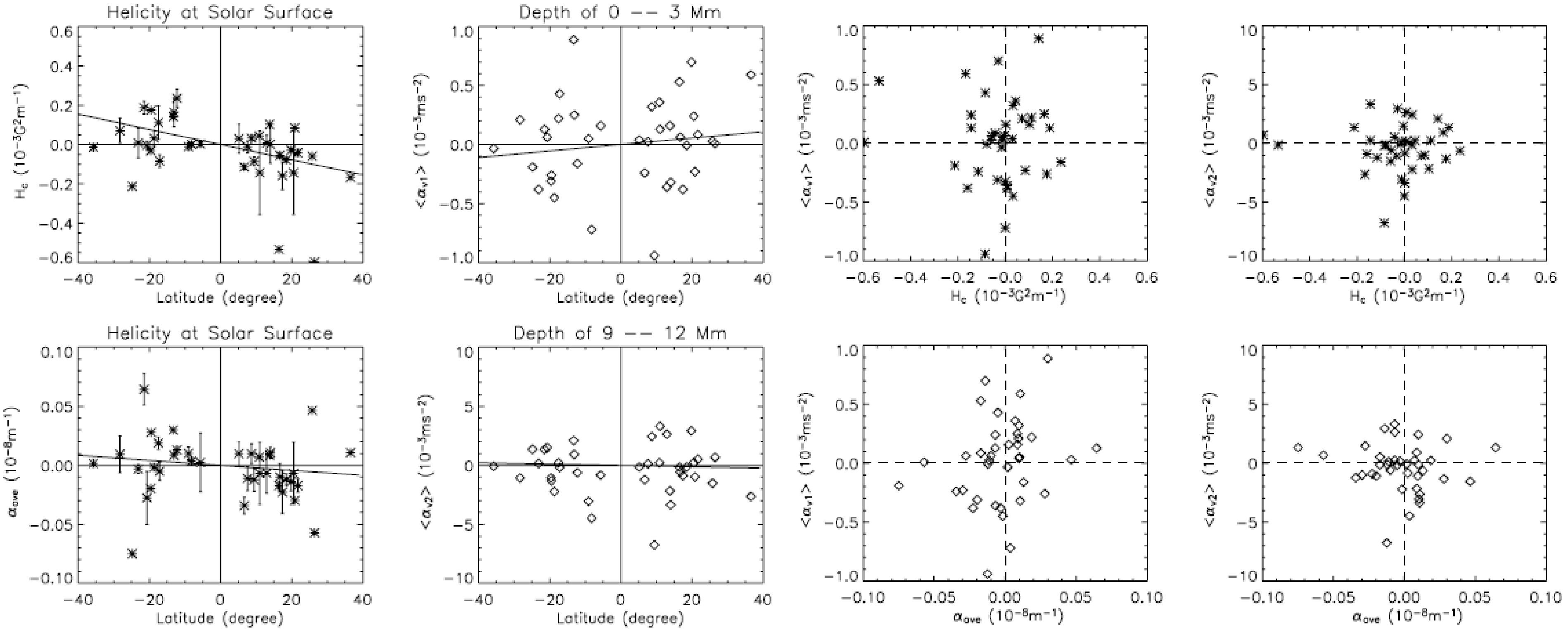

CC: -0.095, 0.118, -0.102, -0.179

Flow Chart for the HMI Time–Distance He lioseismology Data-Analysis Pipeline

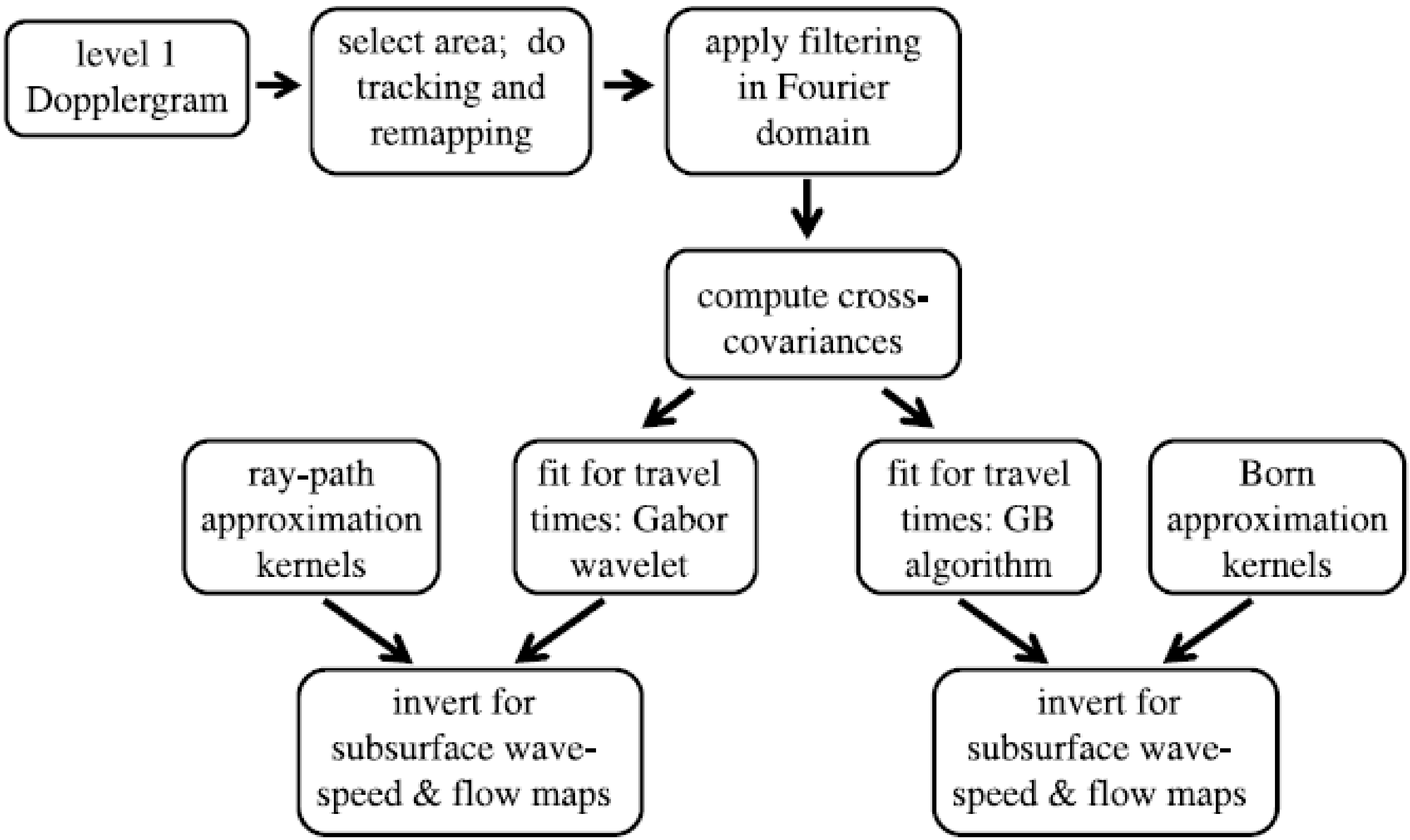

Zhao et al. 2011 Solar Physics.

Observation

SDO/HMI:
Time-series data ;
Vector magnetogram (Schou et al. 2012; Borrero, et al. 2011; Hoeksema et al. 2014; Leka et al. 2009);
Subsurface velocity field of flow (Zhao, 2012) .

NOAA AR11158:
Observed from 10-Feb. 2011 to 16-Feb. 2011.

NOAA AR11283:
Observed from 5-Sep. 2011 to 9-Sep. 2011.

Evolution of Magnetic and Velocity Field

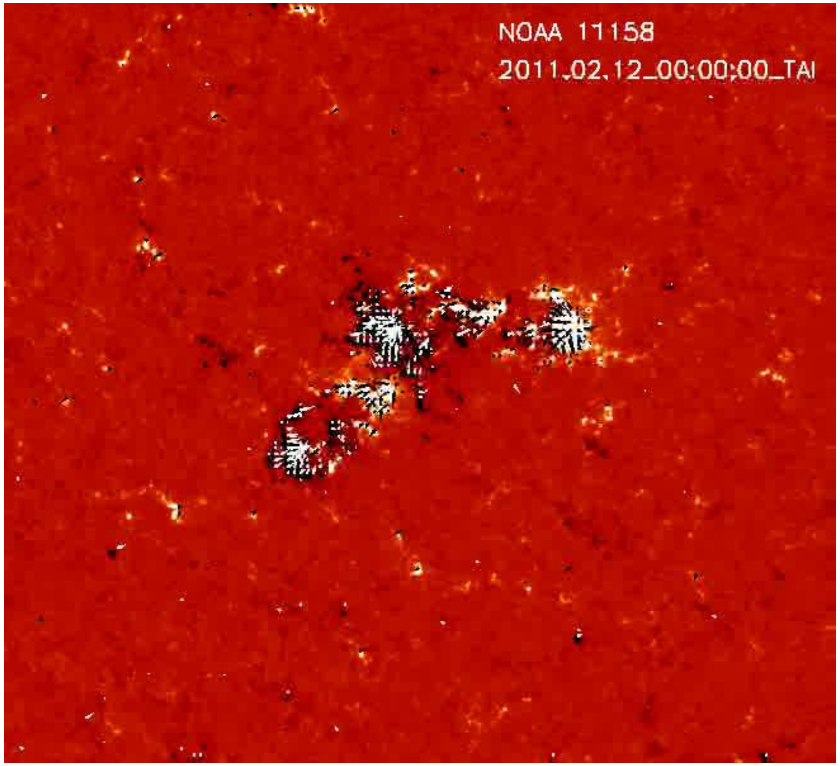

2011-02-15 19:00:00 UT:

FOV: 5.463 ' ×5.043 ';

Resolution: 0.504 ' ';

Cadence: 12 min

Max. $|B_{\perp}|$: 2356 G;

Max. $|B_{//}|$: 2570 G

2011-02-15_14hr:

FOV: 3.04'×2 ';

Resolution: 1.008 ' ';

Temporal Interval: 4 hr;

Max. $|V_{\perp}|$: 441.8 ms^{-1};

Max. $|V_{//}|$: 285 ms^{-1};

Snapshots of Current and Kinetic Helicity

Uncorrelated patterns of between vertical current and kinetic helicities, but the temporal variation of two kinds of helicity showed a relatively clear correlation (shown in next slide);

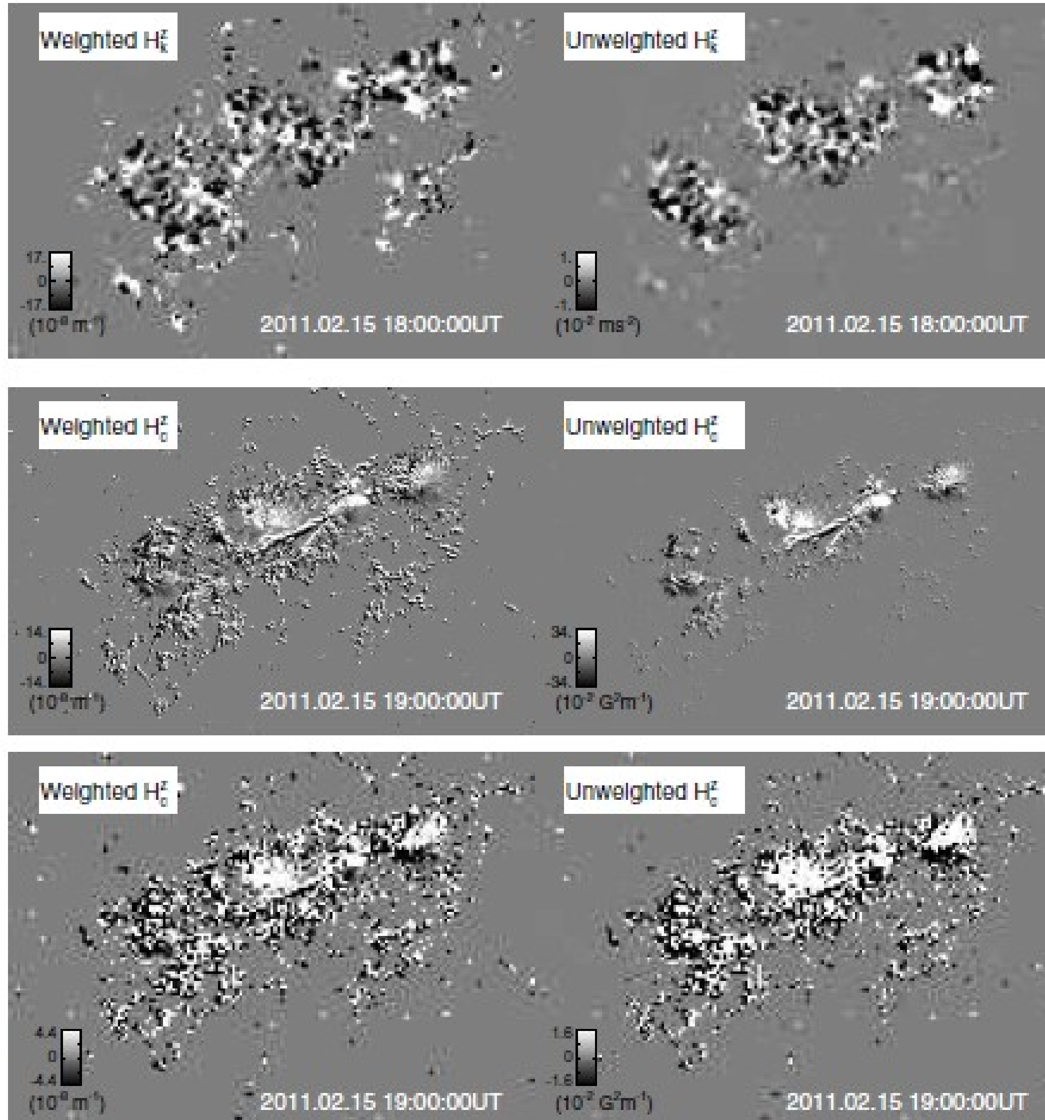

NOAA AR11158 □ Weighted Current Helicity and Kinetic Helicity

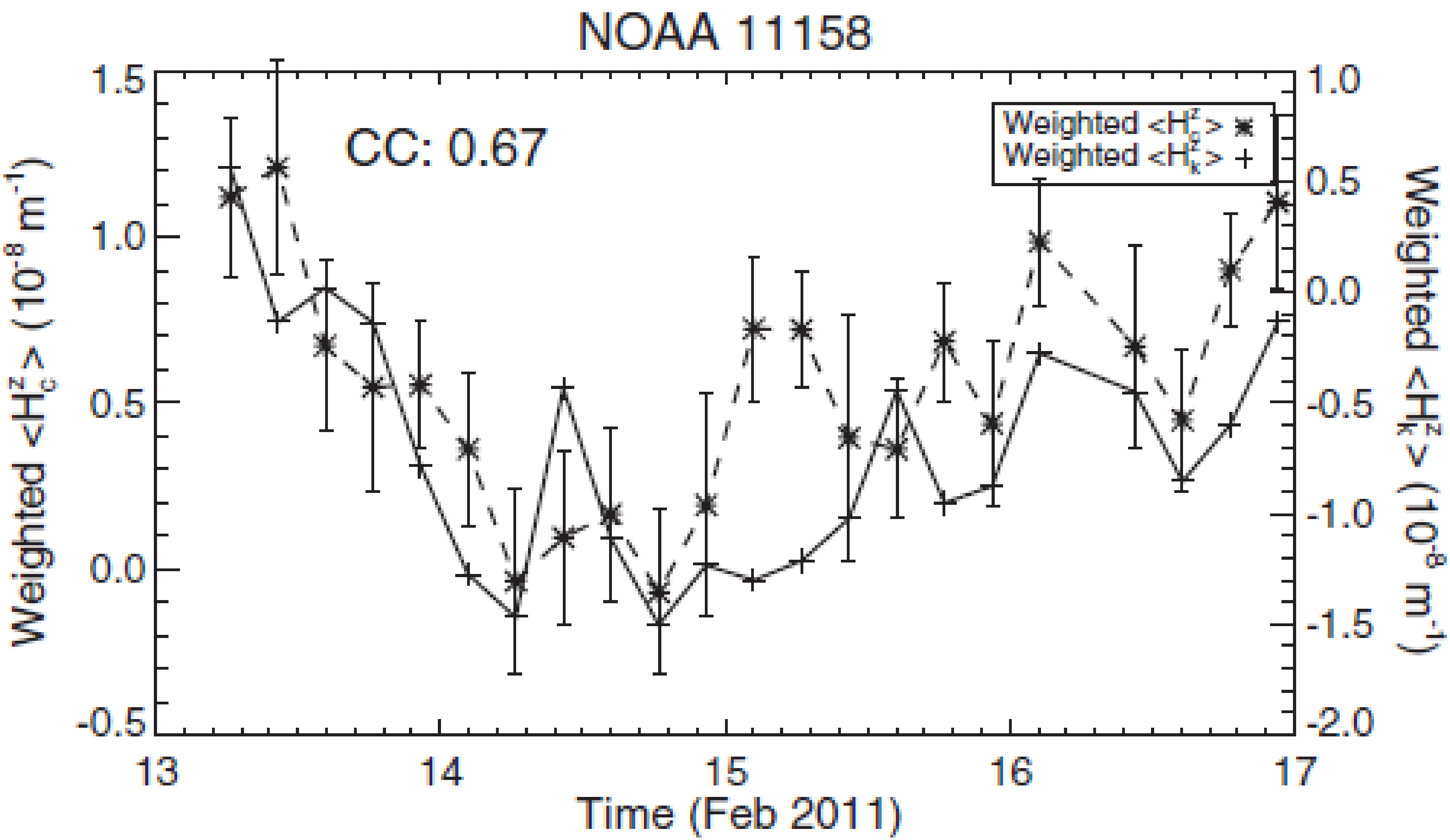

NOAA AR11283 □ Weighted Current Helicity and Kinetic Helicity

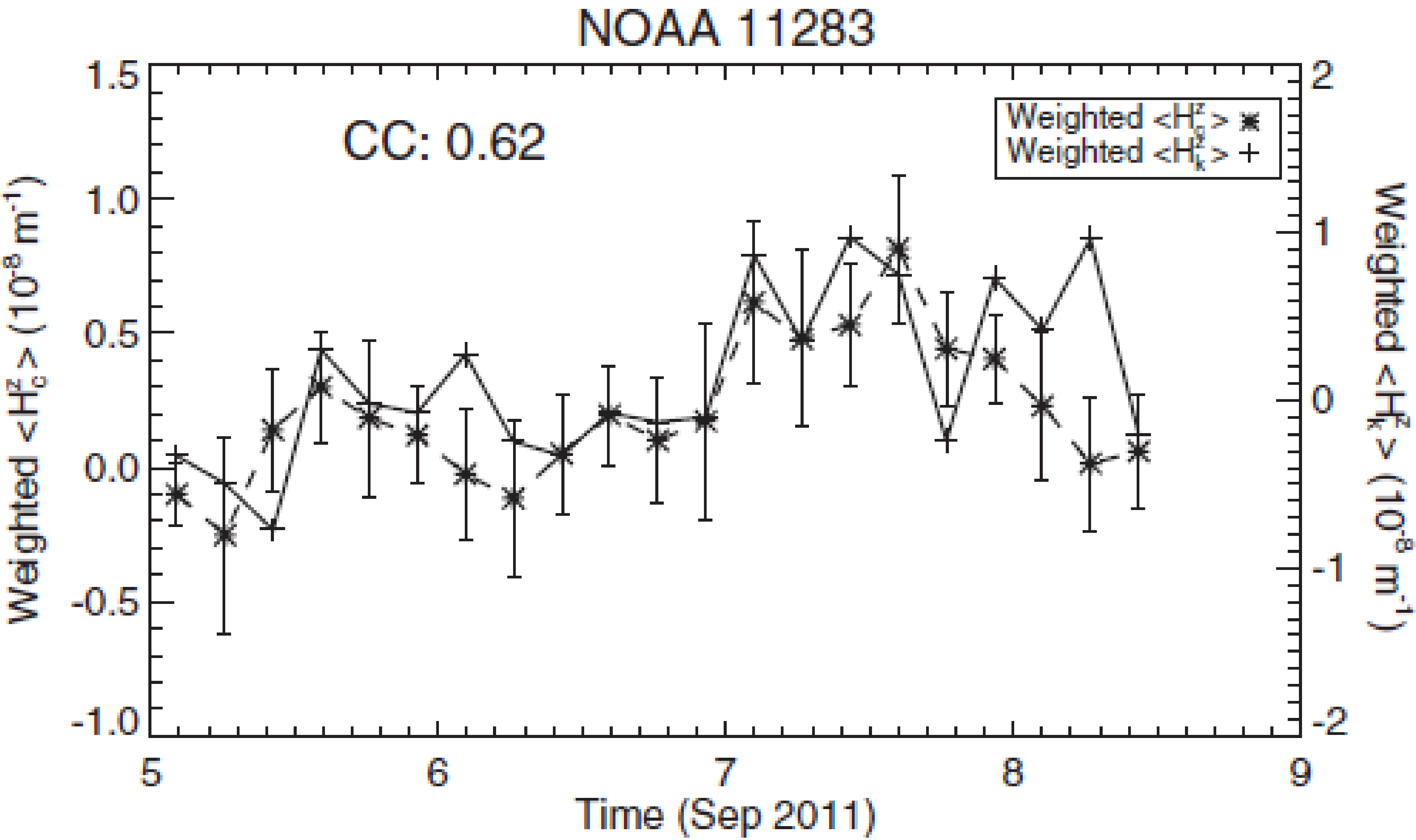

Flare and Subsurface Kinetic Helicity

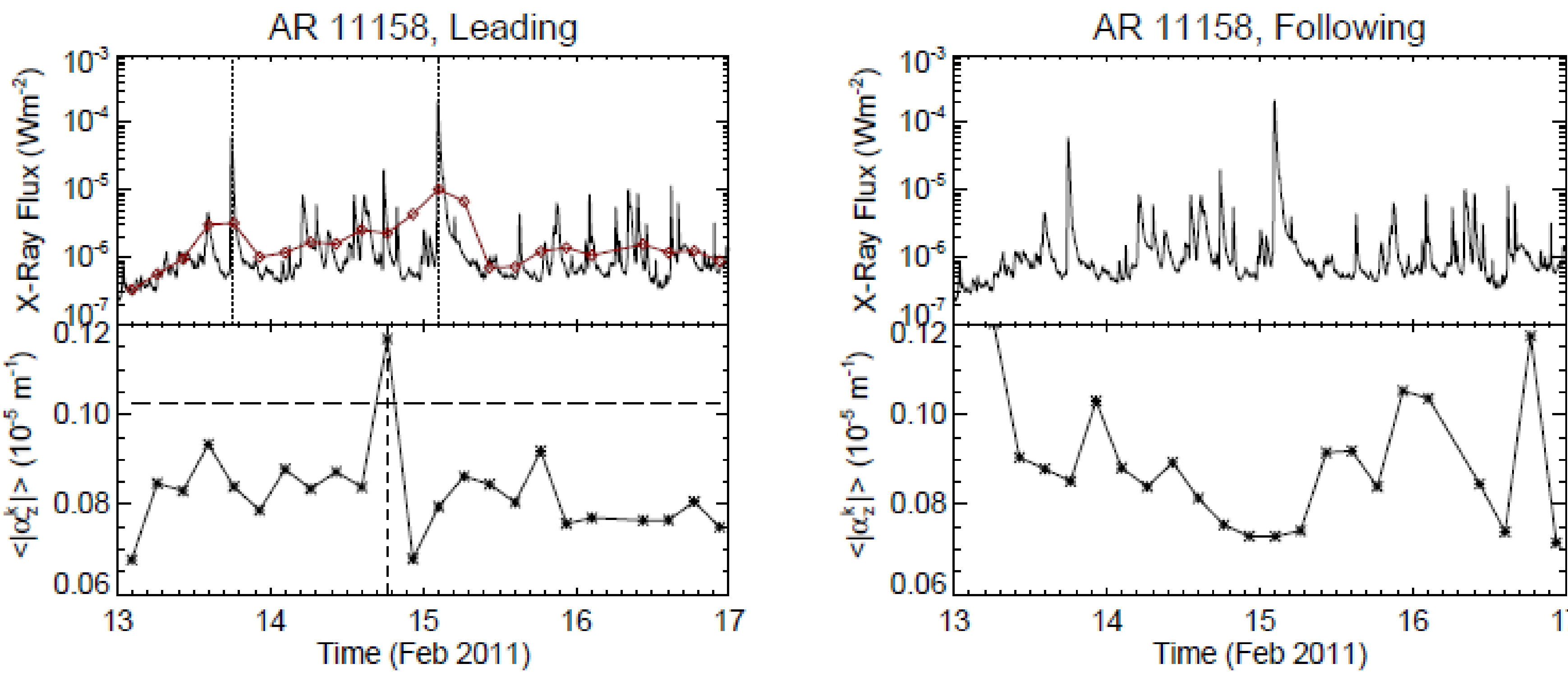

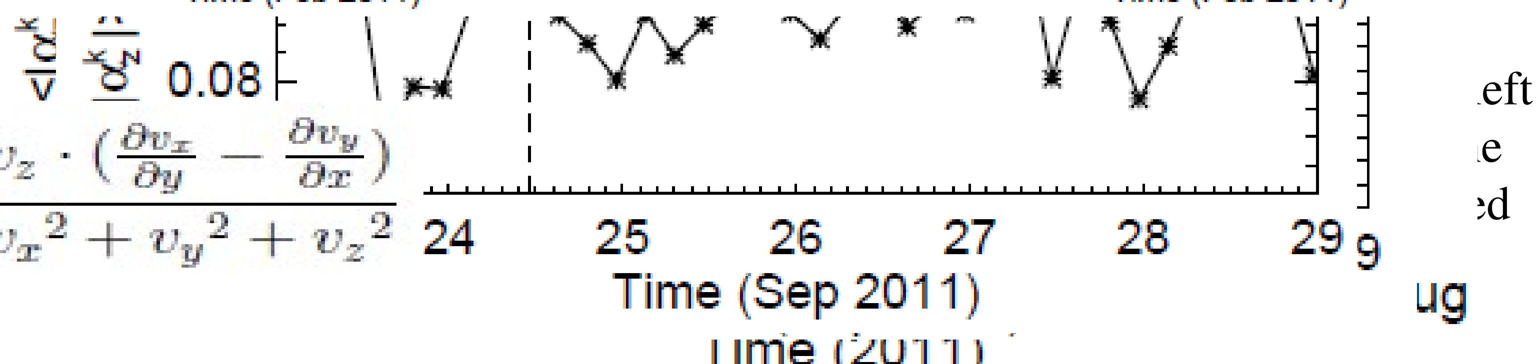

$$\alpha_z^k = \frac{v_z \cdot \left(\frac{\partial v_x}{\partial y} - \frac{\partial v_y}{\partial x}\right)}{{v_x}^2 + {v_y}^2 + {v_z}^2}$$

Systematic Variation or on Occasional Pixels?

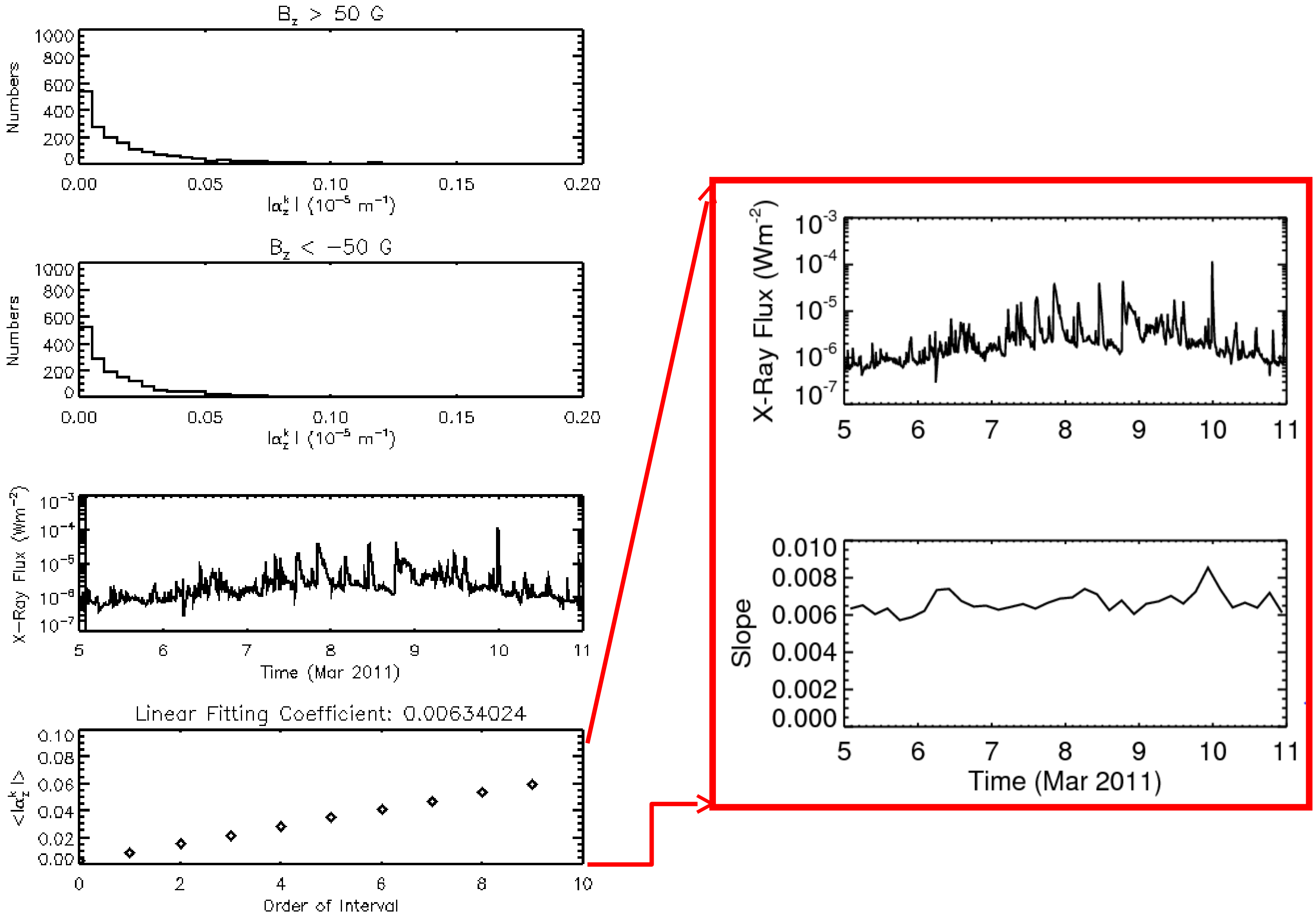

Statistical Study with Subsurface Velocity Field over 24th Solar Cycle

Time period: 2010-04-30 04:00 - 2016-12-27 12:00

Time interval between adjacent group: 8 hrs

Total numbers of vector velocity maps: 36215

Latitude of center: -48°, -24°, 0°, 24°, 48°

Longitude of center: 0°

Field of view: about 5.3'×5.3', (30 ×30 heliographic degree in center of solar disk.)

Match LOS Magnetogram to Velocity Map

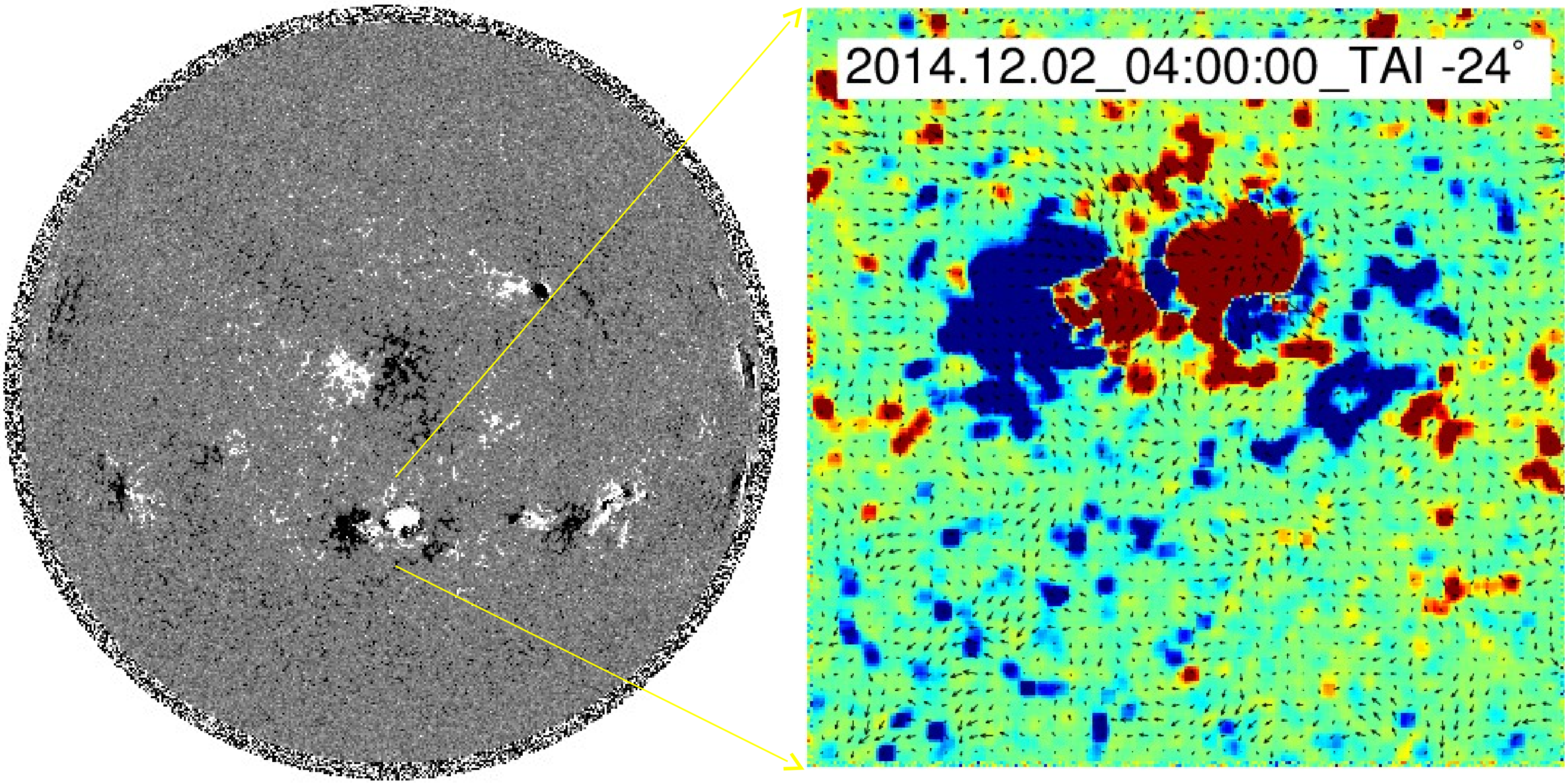

Coordinate systems for solar image data referred to Thompson 2006.
I am grateful to Chou, Dean-Yi; Zhao, Hui ;Yang, Ming-Hsu for the code to align the LOS magnetogram that matches the FOV of velocity map.

Latitude-Time Diagram of Vorticity in 24th Solar Cycle

- Latitude-Time diagram of vorticity exhibits hemispheric sign pref erence.

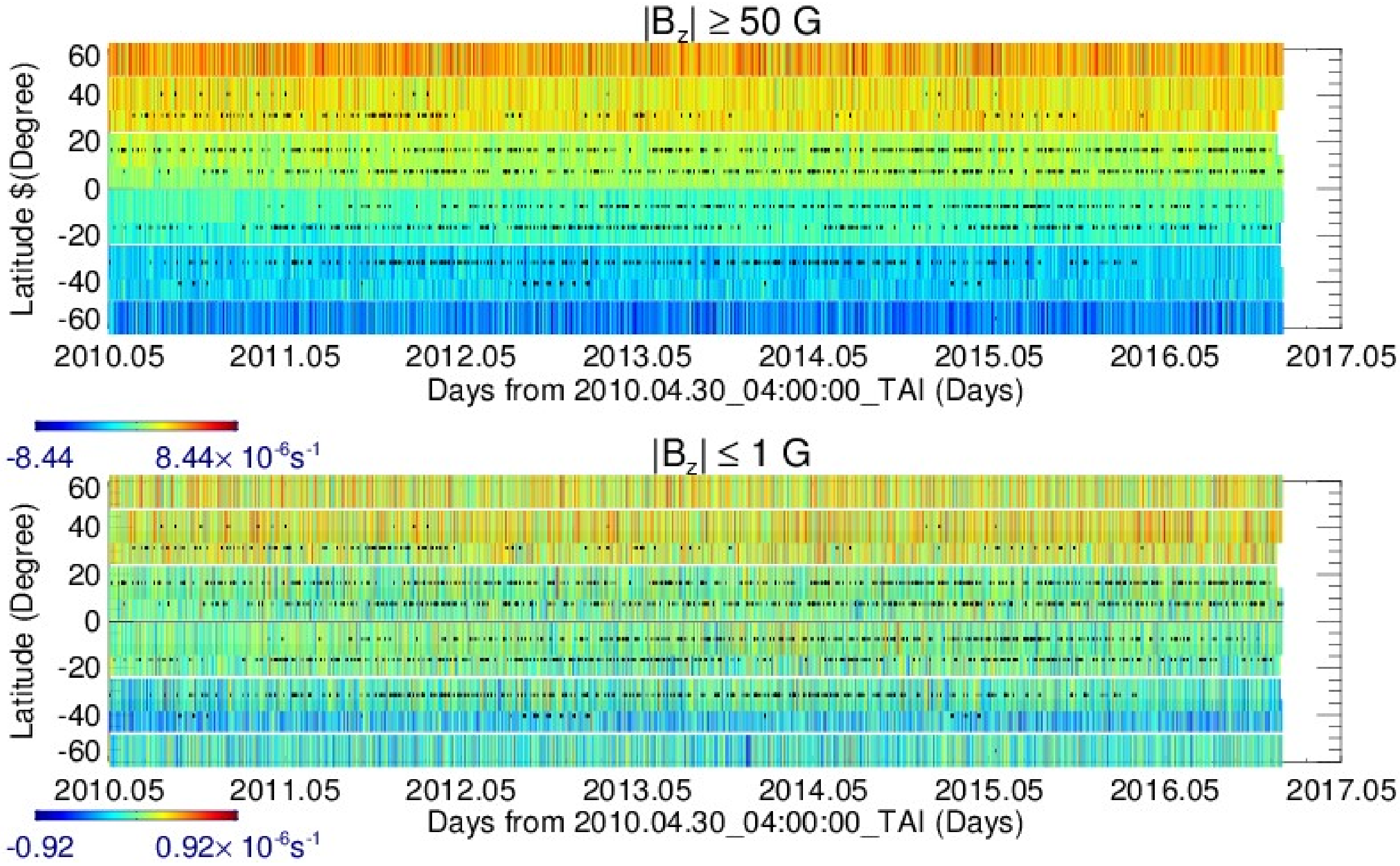

Original Center of FOV ± 7.5 °:

55.5 °
41.5 °
31.5 °
14.5 °
7.5 °
-7.5 °
-14.5 °
-31.5 °
-41.5 °
-55.5°

Hemispheric Sign Preference of Vorticity

Northern Hemisphere (36010) $\omega_z>0$		Southern Hemisphere (36048) $\omega_z<0$	
$\lvert B_z\rvert \geq 50$ G	$\lvert B_z\rvert \leq 1$ G	$\lvert B_z\rvert \geq 50$ G	$\lvert B_z\rvert \leq 1$ G
90.5%	67.7%	91.3%	65.9%

1. Vorticity in active region shows stronger hemispheric sign preference than the current helicity obtained in previous studies.
2. Vorticity shows stronger hemispheric sign preference in region of strong field strength $\lvert B_z\rvert \geq 50$ G than that of weak field strength $\lvert B_z\rvert \leq 1$ G.

Latitude-Time Diagram of Divergence in 24th Solar Cycle

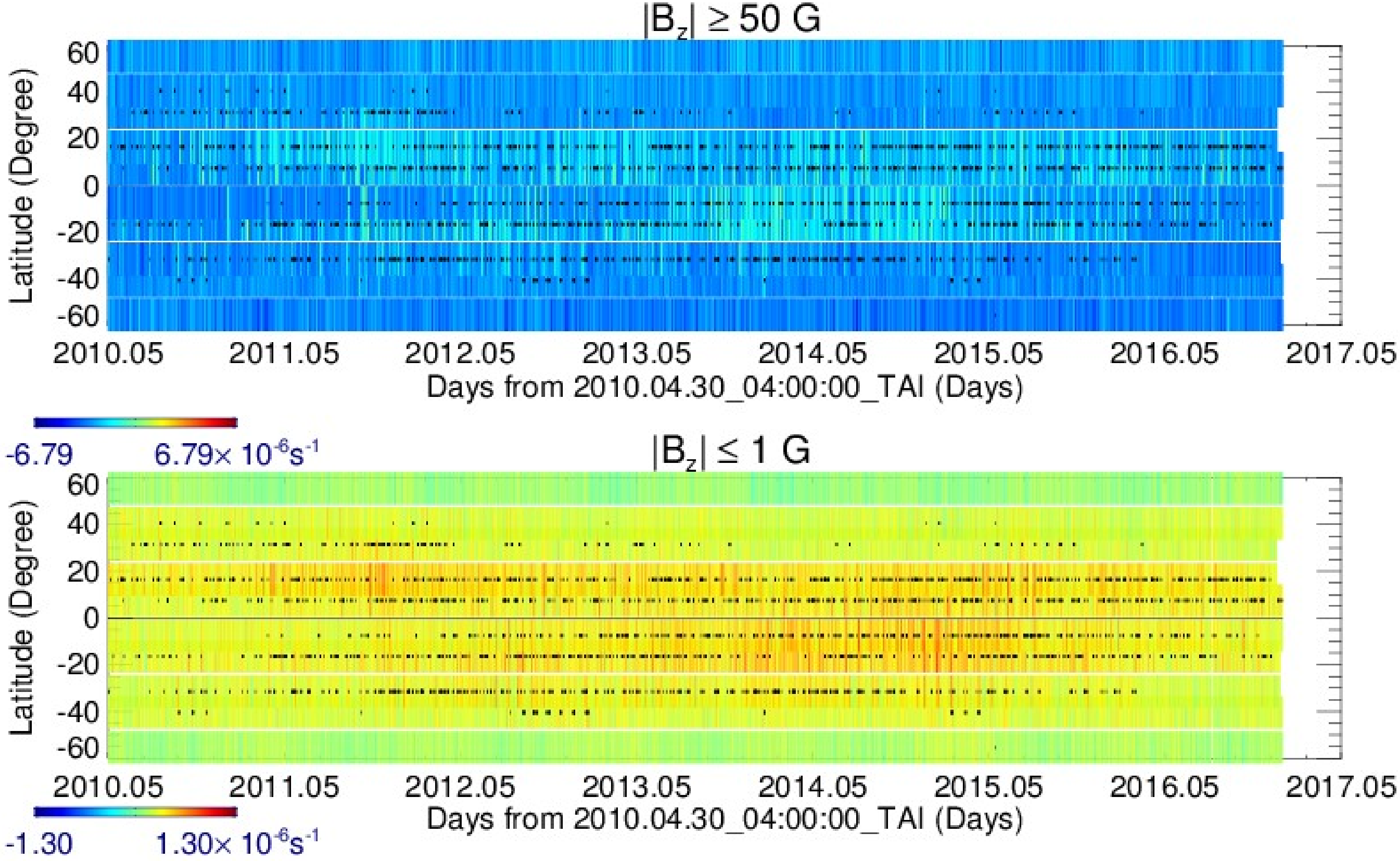

Non-hemispheric but Field-denpendent Sign Preference of Divergence

$\|B_z\| \geq 50$ G (36010) $\langle Div \rangle_z < 0$		$\|B_z\| \leq 1$ G (36048) $\langle Div \rangle_z > 0$	
Northern Hemisphere	**Southern Hemisphere**	**Northern Hemisphere**	**Southern Hemisphere**
99.5%	99.5%	95.5%	97.7%

Divergence shows no hemispheric sign preference but the sign is different in the region between $|B_z| \geq 50$ G and $|B_z| \leq 1$ G.

Yearly Variation Vorticiy

1. Latitudinal profiles of both vorticity and divergence show yearly variation.
2. The latitudinal profiles of divergence show clear N-S asymmetry in the same year.

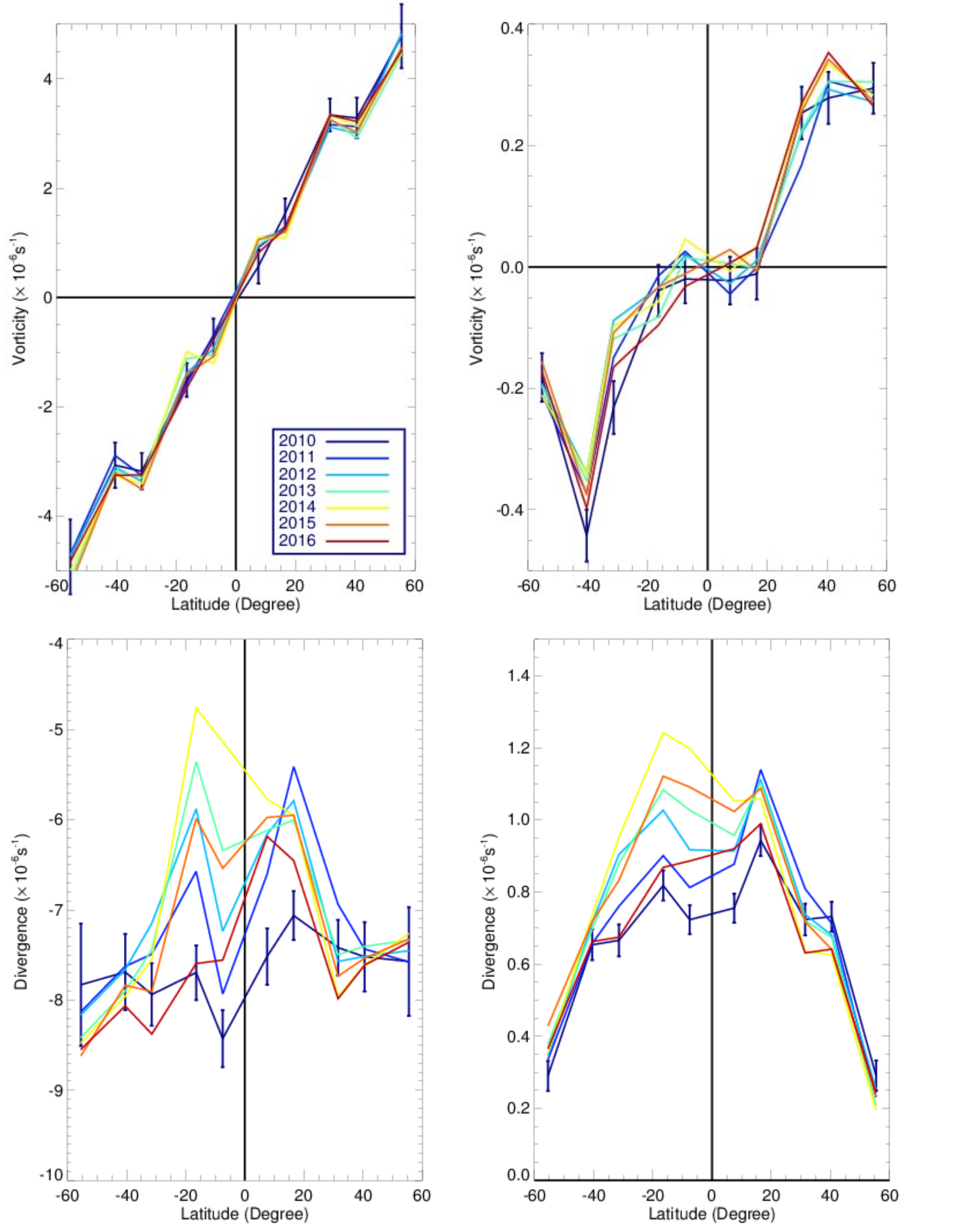

Variation of Latitudinal Profile of Vorticity with Depth (1-3, 3-5, 5-7, 7-9, 9-11 Mm)

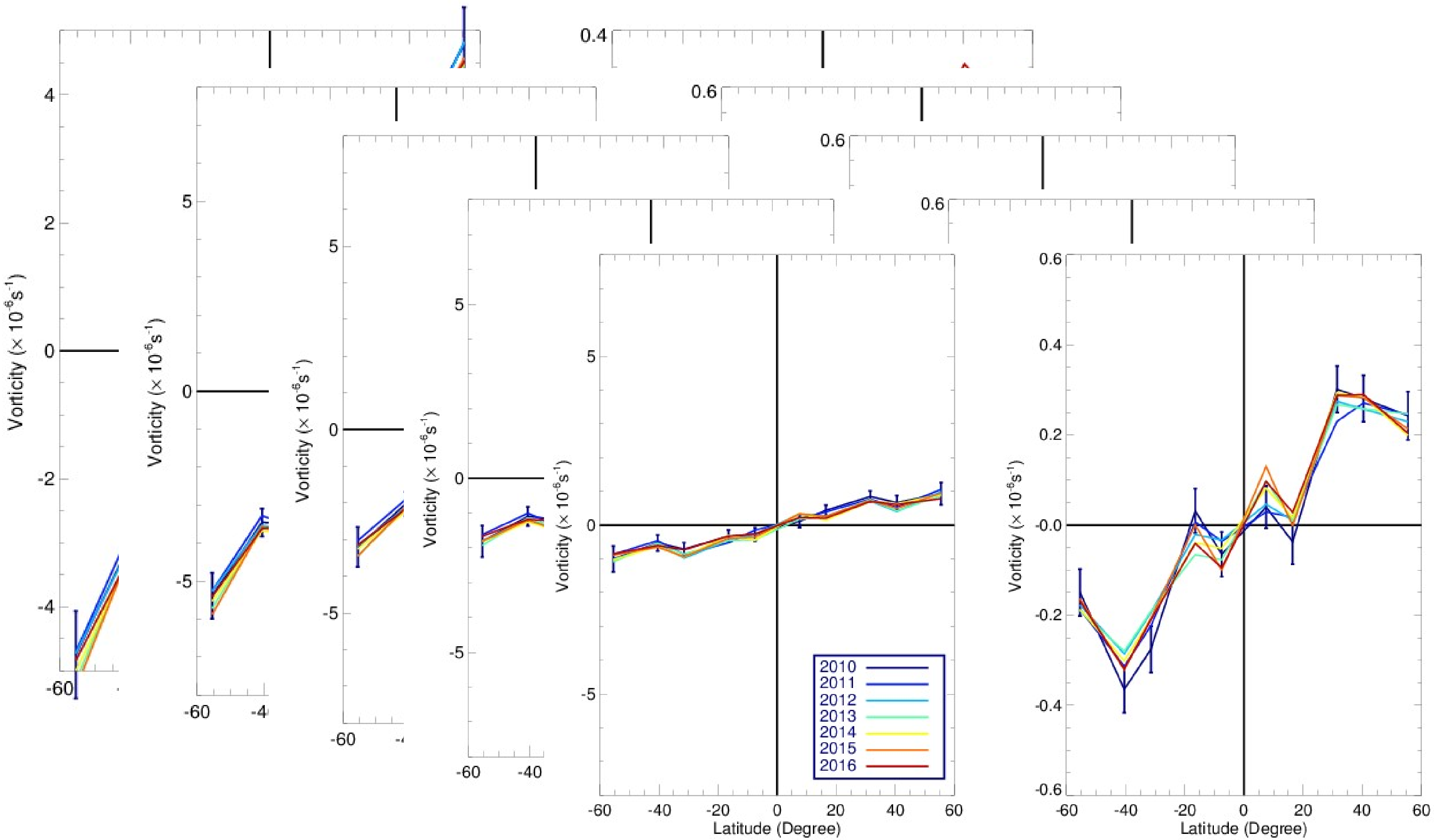

Variation of Latitudinal Profile of Divergence with Depth (1-3, 3-5, 5-7, 7-9, 9-11 Mm)

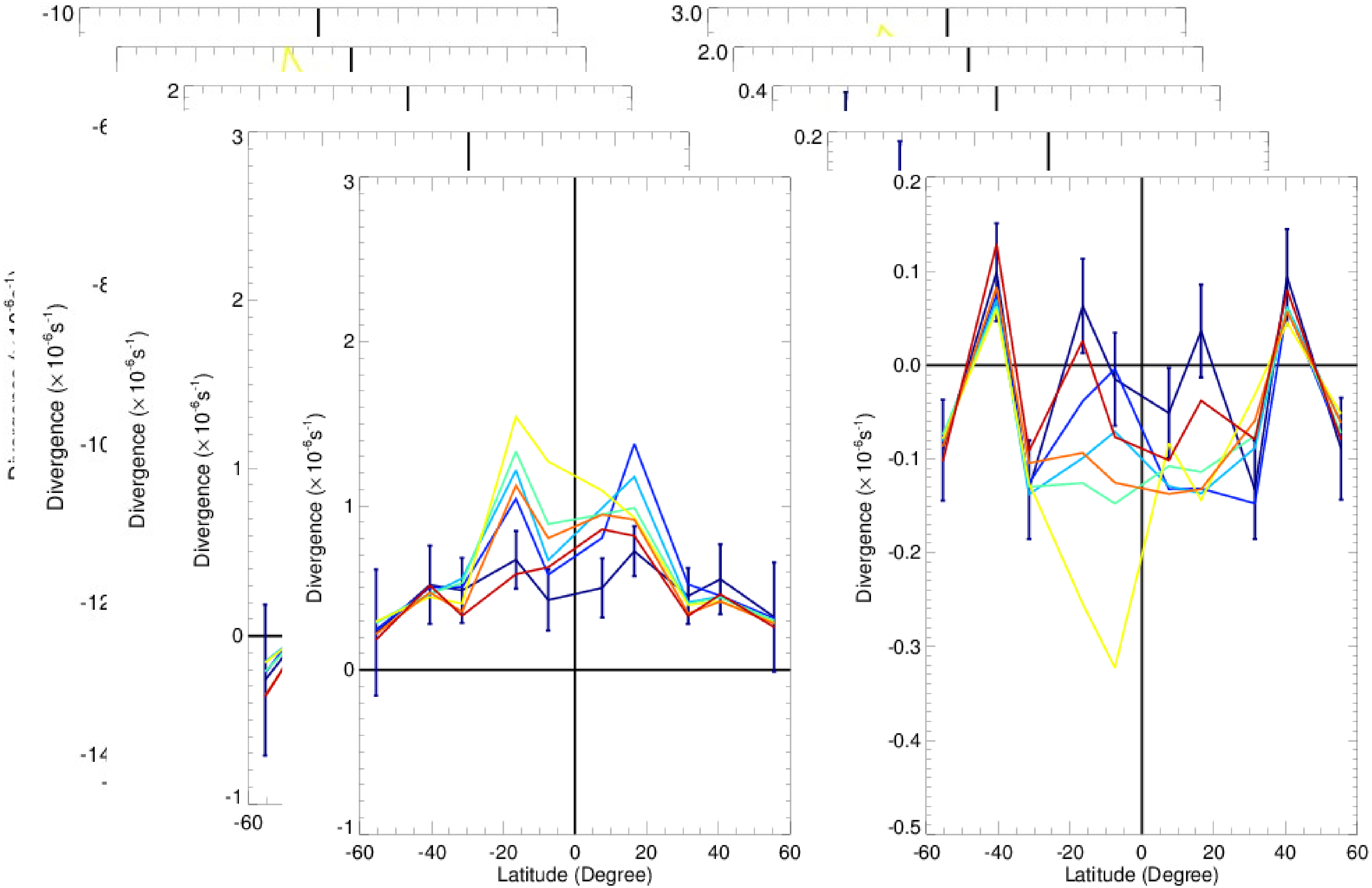

Summary of Main Results

1) Butterfly diagram of current helicity shows mirror asymmetry expected by the mean-field dynamo theory.

2) Connection between the current helicity and subsurface kinetic helicity can be dectected.

3) Subsurface vorticity shows mirror asymmetry too. Meanwhile, the sign of divergence is dependent with the field strength.

4) Yearly variation of vorticity and divergence imply that the buoyancy of flow from the interior of the sun is a way of the energy transportation, furthermore, they behave as prominent North-South asymmetry.

5) Compared with outside ones, latitudinal profile of vorticity and divergence inside the active region keep the shape and sign even in deeper layer. It may imply the dynamical property in active region is more related to the flow in deep layer than its quiet neighborhoods.


Thanks!